Journal of Hazardous Materials 473 (2024) 134605

Contents lists available at ScienceDirect

Journal of Hazardous Materials

journal homepage: www.elsevier.com/locate/jhazmat

# Tracking the history of polycyclic aromatic compounds in London through a River Thames sediment core and ultrahigh resolution mass spectrometry

Rory P. Downham [a], Benedict Gannon [a], Diana Catalina Palacio Lozano [a], Hugh E. Jones [a], Christopher H. Vane [b], Mark P. Barrow [a,*]

[a] Department of Chemistry, University of Warwick, Coventry CV4 7AL, UK
[b] British Geological Survey, Organic Geochemistry Facility, Keyworth NG12 5GG, UK

## HIGHLIGHTS

- A Thames sediment core was measured using ultrahigh-resolution mass spectrometry.
- Untargeted analysis revealed complex contributions from polycyclic aromatic compounds.
- Polycyclic aromatic compounds included oxygen, sulfur, nitrogen, and chlorine atoms.
- A maximum of 1676 polycyclic aromatic molecular components seen for one core depth.
- Temporal polycyclic aromatic compound variations likely reflect coal consumption.

## GRAPHICAL ABSTRACT

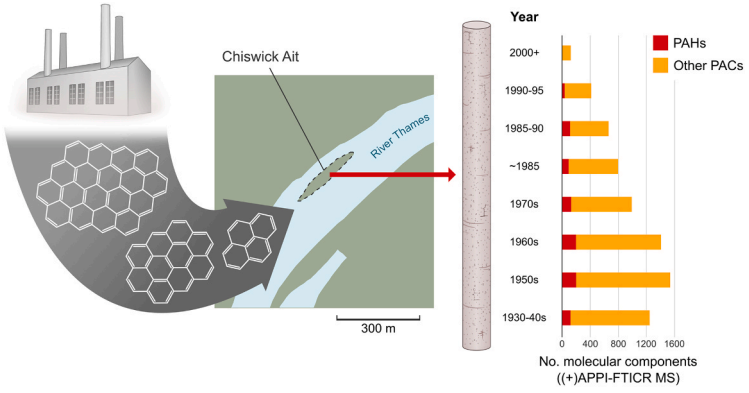


## ARTICLE INFO

*Keywords:*
Polycyclic aromatic compounds (PAC)
Polycyclic aromatic hydrocarbons (PAH)
Ultrahigh resolution mass spectrometry
Fourier transform ion cyclotron resonance mass spectrometry (FTICR MS)
Contamination

## ABSTRACT

Polycyclic aromatic compounds (PACs), including polycyclic aromatic hydrocarbons (PAHs) and heteroatom-containing analogues, constitute an important environmental contaminant class. For decades, limited numbers of priority PAHs have been routinely targeted in pollution investigations, however, there is growing awareness for the potential occurrence of thousands of PACs in the environment. In this study, untargeted Fourier transform ion cyclotron resonance mass spectrometry was used for the molecular characterisation of PACs in a sediment core from Chiswick Ait, in the River Thames, London, UK. Using complex mixture analysis approaches, including aromaticity index calculations, the number of molecular PAC components was determined for eight core depths, extending back to the 1930s. A maximum of 1676 molecular compositions representing PACs was detected at the depth corresponding to the 1950s, and a decline in PAC numbers was observed up the core. A case linking the PACs to London's coal consumption history is presented, alongside other possible sources, with some data features indicating pyrogenic origins. The overall core profile trend in PAC components, including compounds with oxygen, sulfur, nitrogen, and chlorine atoms, is shown to broadly correspond to the 16 priority PAH concentration profile trend previously determined for this core. These findings have implications for other industry-impacted environments.

* Corresponding author.
*E-mail address:* M.P.Barrow@warwick.ac.uk (M.P. Barrow).

https://doi.org/10.1016/j.jhazmat.2024.134605
Received 7 March 2024; Received in revised form 27 April 2024; Accepted 11 May 2024
Available online 14 May 2024

## 1. Introduction

The reliance on coal in London for domestic heating and power generation led to prominent smog events between the late 1700s through to the 1960s [1,2]. The most severe event, 'the Great Smog of London' of 1952, caused an estimated 12,000 deaths [2,3]. This prompted the Clean Air Act of 1956 (revisited in 1968) [1–3], driving a change away from coal reliance in cities towards smokeless fuels through the decades that followed [4].

Understanding the impact of industrialisation and urbanisation on the environment is of high and ongoing importance [5,6], and assessing environmental matrices for toxicity plays a key role in meeting this challenge. As contaminant reservoirs, soils and sediments can represent useful archives for the study of spatial and temporal variations in pollution [7,8]. Monitoring soils and sediments for toxicity is of further importance due of the risk of pollutant release upon disturbance, for instance, during severe weather events or engineering activities [7,9].

Environmental monitoring involves determining the concentrations of priority pollutants, such as polycyclic aromatic hydrocarbons (PAHs), in various matrices [10,11]. The PAH compound group has been a particular focus in environmental science since 16 PAHs were specified as priority targets by the U.S. Environmental Protection Agency (USEPA) in 1976 [9,12,13]. PAHs feature two or more aromatic rings fused together [9,14], with naphthalene being the simplest example [15]. Various priority PAHs are recognised or suspected to be carcinogenic, mutagenic and / or teratogenic [16–18], with some also demonstrated to be endocrine disruptors [19,20].

Terrestrially, PAHs are created through the diagenesis processes associated with fossil fuel formation [21]. They are also products of biogenic transformation processes, and the pyrolysis or incomplete combustion of fossil fuels and other organic matter, including vegetation [17,22,23]. Natural PAH emissions are considered minor compared to anthropogenic contributions [11,14,18], of which incomplete fuel combustion from domestic activities, vehicle use, and industry is thought to be particularly significant [22,24,25].

Hundreds of PAHs have been identified [16,26], and it is recognised that PAHs often occur in complex mixtures of isomers rather than as isolated compounds [9,18,22]. Human exposure to PAH mixtures in the environment has hence attracted recent attention [11,27,28]. Indeed, in 2015, Andersson and Achten highlighted that environmental assessments based around the USEPA 16 priority PAHs likely underestimate toxicity, especially for fossil fuel contamination scenarios [12].

Environmental samples may also contain heterocyclic PAH analogues [29] and heteroatom-substituted PAH derivatives [12]. These are compounds with similar configurations of fused aromatic rings, but with the inclusion of one or more nitrogen, sulfur, and / or oxygen atoms, or PAHs with substituent groups containing these heteroatoms [12,30,31]. Together with PAHs, these NSO-heterocycle and NSO-substituted compounds belong to the broader polycyclic aromatic compound (PAC) class [12,30], and are also released into the environment from combustion sources [32–34]. In addition, NSO-PACs may form following the microbial or photolytic degradation of PAHs, and following reactions between PAHs and pollutant gases, including nitrogen oxides, ozone, and sulfur dioxide [12,24,34,35]. It is important to also acknowledge that some PACs may also be regarded as asphaltenes, which represent a highly complex operational fraction of crude oil and coal, usually defined in terms of solubility in aromatic solvents and insolubility in low-molecular-weight n-alkanes [36]. Asphaltenes can be described in terms of a PAC core with alkyl side chains, or multiple PAC cores bridged by alkyl chains [37–39].

The common occurrence of various heteroatom-containing PACs in the environment is now recognised [12]. Extended target lists of PAHs with additional heteroatom-containing PACs have been used in multiple sediment core studies around the world, to evaluate the impact of changing fossil fuel usage, or the onset of specific industrial activities [34,40–42]. Recently, Chibwe et al. studied a lake sediment core in the Athabasca oil sands region, Canada, deploying a more advanced, untargeted two-dimensional GC–time-of-flight MS approach alongside targeted analysis for PAC measurements [43]. In this way, Chibwe et al. tracked core profile changes for over 100 heteroatom-containing PACs and observed an exponential increase in PAC deposition coinciding with oil sands operations in the region [43].

Fourier transform ion cyclotron resonance (FTICR) mass spectrometry provides one of the most effective approaches for untargeted screening analysis [44]. FTICR mass spectrometry is established for the molecular characterisation of complex natural mixtures, such as crude oils and natural organic matter, which have been shown to contain thousands, to hundreds of thousands of molecular components [45,46]. The analysis of these complex mixtures is possible due to the unparalleled resolving power achievable with FTICR mass spectrometry, which enables high mass accuracy, and consequently, high-confidence molecular formulae assignments [47,48]. The molecular characterisation of complex mixtures is routinely achieved via direct infusion FTICR mass spectrometry, with soft ionization sources, including electrospray ionization (ESI) and atmospheric pressure photoionization (APPI) [44,48].

Visualisation strategies for representing complex mixture mass spectra follow from categorising the assigned molecular formulae in terms of compound class, carbon number, and double bond equivalents (DBE) [48,49]. The latter represents the number of rings and double bonds involving carbon (see equation 1) [49,50]. Then, plots such as compound class distributions, and DBE versus carbon number heat maps, can be generated. These are particularly useful for understanding compositional differences between complex samples.

Recent Fourier transform (FT) mass spectrometry-based studies, deploying Orbitrap or FTICR instruments in an untargeted capacity, have provided further insights into the range of PACs occurring in the environment. Luo and Schrader analysed dichloromethane Soxhlet extracts of a highly contaminated soil from an industrial site in Germany, via direct-infusion FT Orbitrap mass spectrometry [44]. Taking advantage of complementary ionization techniques, including ESI, APPI and atmospheric pressure chemical ionization (APCI), Luo and Schrader detected thousands of PAHs and heteroatom-containing PACs, with distributions extended to much greater molecular weights and DBE than the routinely reported priority compounds [44]. Various other studies have shed light on the complex mixtures of PACs occurring in atmospheric aerosols via FT Orbitrap MS [51] and FTICR MS [52–56].

In the present work, an FTICR MS approach was employed to analyse a sediment core from Chiswick Ait; the most downstream island in the tidal River Thames. Chiswick Ait is within London's urban reaches and represents a study site with relatively undisturbed sediments, containing a local pollution record [4,7]. In a recent study, Vane et al. revealed changes through the profile of the same sediment core in priority PAHs and total petroleum hydrocarbons (TPH), along with other pollutant compounds and markers, from the 1930s to the modern day [4]. The aim of the FTICR MS approach used in the present study was to gain further insights into anthropogenic organic matter contributions to the sediments. The broadband, untargeted screening approach revealed prominent PAC distributions, exhibiting temporal variance that is likely reflective of London's history of coal use since the 1930s. The trends in these PAC distributions are compared to the 16 USEPA PAH concentration trend determined in the previous research [4].

## 2. Experimental

### 2.1. Sediment core collection and sample preparation

Sediment cores were collected from Chiswick Ait in the inner Thames estuary, London, UK, in March 2018, as published by Vane et al. [7]. All samples analysed via FTICR MS herein were from core B, retrieved from a transect (51° 29′13.4" N, 0° 14′48.18" W to 51° 29′17.1" N, 0 ° 14′ 41.64" W) as described previously [7]. The core was sectioned continuously at 5 cm intervals for the depth range 0 to 20 cm, and at 10 cm

intervals for the depth range 20 to 60 cm, thus generating eight samples. All samples were freeze-dried, sieved (< 2 mm mesh) and ground using a ball mill (< 200 μm).

Sediment samples (2 g) were mixed with sodium sulfate and copper powder for extraction in dichloromethane (Fisher Scientific, Hemel Hempstead, Hertfordshire, UK) via accelerated solvent extraction (ASE, Dionex-300). ASE was conducted at 100 °C and 1500 psi, with a 5 min heat-up phase followed by a static 10 min extraction. Extracts were subsequently reduced to approximately 5 mL under nitrogen gas, and then filtered using Whatman GF/F glass microfiber filters (GE Healthcare, Lifesciences, Pittsburgh, USA).

A total of eight sediment extracts were prepared (as above) for FTICR mass spectrometric analysis (see Table 1). The sediment chronology was determined and reported in detail previously [7]. In brief, this entailed using a combination of time markers including short lived radioactive isotope $^{137}$Cs (related to the atmospheric testing of nuclear weapons) as well as Pb ratios ($^{207/206}$Pb), and the rise and fall of banned persistent organic pollutants (such as polychlorinated biphenyls) [7]. These data provided approximate decade ranges for the sample depths.

### 2.2. FTICR MS

Subsamples of the sediment extracts were diluted with a 50:50% v/v solvent mixture of propan-2-ol (HPLC grade, Sigma Aldrich, Haverhill, Suffolk, UK) and toluene (HPLC grade, Honeywell, Basingstoke, Berkshire, UK), for direct infusion analysis using a 12 T solariX FTICR mass spectrometer (Bruker Daltonik GmbH, Bremen, Germany). Samples were introduced via an APPI II source (Bruker Daltonik GmbH, Bremen, Germany) with a flow rate of 600 μL/h. The source vaporizer was maintained at 350 °C, the nitrogen nebulizing gas pressure was 1.3 bar, and the nitrogen drying gas was set to 4.0 L/min and 230 °C. Ionization was achieved using the in-source krypton lamp, emitting photons at 10.0 eV and 10.6 eV. The instrument was operated in positive-ion mode (hence '(+)APPI'), with the transfer capillary held at a potential of −2000 V.

Ions were accumulated in a collision cell for 0.2 s before being transferred to the infinity cell analyser, where ions were detected over a range of *m/z* 150 – 3000. Each sample mass spectrum represents a summed dataset of 300 coadded scans of 4 million data points, subsequently zero-filled, apodised, processed via the fast Fourier transform, and plotted in magnitude mode. The resolving power achieved was approximately 450,000 FWHM, at *m/z* 400.

The mass spectra were externally calibrated [57] with sodium trifluoroacetate (98%, Aldrich, UK) solution (50:50% v/v toluene and methanol, HPLC grade, Honeywell, Basingstoke, Berkshire, UK). A mass spectrum of a sediment extract doped with sodium trifluoroacetate was also acquired, and internally recalibrated [57] against dopant peaks. A calibration list was subsequently created from $O_3$[H] and HC[H] class homologous series (Table S1, supplementary information) for internally recalibrating all (+)APPI sample spectra, using DataAnalysis 5.0 (Bruker Daltonik GmbH, Bremen, Germany).

The sediment extracts were further analysed using the 12 T FTICR mass spectrometer via nano electrospray ionization, with operation in negative-ion mode ('(-)nESI'), to access more polar compositions not detectable via APPI. Experimental details and focused results for the (-)nESI measurements have been included in the supplementary information.

**Table 1**
Sediment sample depths and corresponding core chronology (see Vane et al. [7]).

| Sample depth /cm | Approximate chronology |
|---|---|
| 2.5 | 2000+ |
| 7.5 | 1990-1995 |
| 12.5 | c.1985-1990 |
| 17.5 | c.1985 |
| 25 | 1970s |
| 35 | 1960s |
| 45 | 1950s |
| 55 | 1930-1940s |

### 2.3. Data analysis

Following internal recalibrations, (+)APPI-FTICR mass spectra were exported for processing in Composer 1.5.6 (Sierra Analytics, Modesto, CA, USA). Peaks present in ASE, filter paper, and solvent blank FTICR mass spectra, at > 1% base peak intensity, were subtracted from sediment sample mass spectra. Sample peaks were then assigned molecular formulae within a matching tolerance of 1 ppm, by searching for homologous series (molecular progressions with $CH_2$ building units) using the elemental constraints: C = 0–200, H = 0–1000, O = 0–12, S = 0–2, N = 0–2, P = 0–1, Cl = 0–2. The root-mean square errors were < 0.35 ppm for the resultant assigned (+)APPI data sets, which were subsequently processed using the in-house KairosMS software (University of Warwick, Coventry, UK) for further analyses and data visualization treatments [58], as per recent studies [36,59,60]. This included generating DBE versus carbon number plots for the compound classes, with DBE calculated in accordance with equation 1 [49,50].

Equation 1:

$$DBE = 1 + C - \frac{(H + X)}{2} + \frac{(N + P)}{2}$$

where C, H, N, P and X are the numbers of carbon, hydrogen, nitrogen, phosphorus, and halogen atoms in a molecular formula, respectively.

Aromaticity index (AI) was calculated for all assigned molecular formulae (neutral analytes), using equation 2 [61,62], to estimate the PAC contributions in the samples. AI values > 0.5 represent aromatic compounds, and values ≥ 0.67 represent condensed aromatics [61,62], hence PACs are approximated by the latter [63,64]. The modified aromaticity index ($AI_{mod}$) was not employed in this work, because it is unknown whether the carboxyl group assumption is valid for these samples [61,62]. Similarly, the more conservative reformulated aromaticity index (rAI) and modified version ($rAI_{mod}$) [65] were not adopted, as these may be more appropriate if non-condensed cyclic carbonyl compounds are anticipated to be significant components. It is worth noting that these equations provide the same values for pure hydrocarbons. A comparison between AI, $AI_{mod}$, rAI and $rAI_{mod}$ for the sample predicted to contain the highest number of oxygen-containing PACs by AI has been included in Fig. S1, supplementary information.

Equation 2:

$$AI = \frac{1 + C - O - S - 0.5(H + N + P + X)}{C - O - N - S - P}$$

where C, O, S, H, N, P and X are the numbers of carbon, oxygen, sulfur, hydrogen, nitrogen, phosphorus, and halogen atoms in a molecular formula, respectively. The inclusion of halogen atoms in equation 2 is consistent with work by Wang et al. [63].

## 3. Results and discussion

### 3.1. Overall trends in compositions

The assigned molecular formulae for the eight (+)APPI sediment depth datasets were categorised by compound class, as shown in the compound distribution in Fig. 1. The classes are represented with heteroatom counts, e.g., $O_1$ represents all organic compounds with exactly one oxygen atom and $S_1$ represents all formulae with one sulfur atom (N. B. HC refers to pure hydrocarbons). Classes with '[H]' denote protonated ion species in positive-ion mode, whereas the others represent radical cations – both are generated via (+)APPI, and each sample analyte has the potential to generate both ion species [66,67]. Fig. 1 shows the

number of monoisotopic molecular components per class for each sediment extract, expressed as a percentage of the total number of monoisotopic components assigned in those extracts. Only compound classes with an overall signal contribution above 1% (for monoisotopic assignments) in at least one sample have been included in the class distribution and subsequent data analyses.

The compound class distribution provides an overview of the changes to the chemical composition of the sediment core as a function of depth. The hydrocarbon classes, HC and HC[H], show a general, increasing trend in component contributions down the sediment core, with a decrease at the bottom level (Fig. 1). Although PAHs cannot be directly inferred from the HC and HC[H] classes in the distribution plot, it is interesting that a similar core profile trend was demonstrated for the 16 USEPA PAH concentrations by Vane et al. [4] The radical oxygenated classes, $O_1$–$O_4$, also follow a very similar pattern to the HC class in the (+)APPI-FTICR MS data, with increasing contributions down the sediment core and a decrease for the 55 cm depth. Other heteroatom classes exhibiting similar profile patterns, but more minor contributions overall, include $O_1S_1$, $O_1S_1$[H], $N_1$ and $N_1O_1$. The $S_1$ class, often of interest for potential fossil fuel markers [32,68,69], was similar in percentage component contributions to the $O_1S_1$ class for the 35 and 45 cm sample depths, but was much diminished for the rest of the sediment core. The 35 and 45 cm depths were shown to be the most PAH-contaminated for the core in the study by Vane et al. (Σ16 USEPA PAH 70.9 and 98.5 mg/kg$^{-1}$, respectively), and the 35 cm depth was also highest in total petroleum hydrocarbon concentrations [4].

### 3.2. PAC speciation and numbers of molecular PAC components by depth

The numbers of PAC molecular components, defined by AI $\geq$ 0.67, assigned for each core depth in the (+)APPI data, are displayed in Fig. 2. The data have been presented in terms of different compound classes or class groups, and show how some classes, e.g. $S_1$-PACs, were only ionized as radical ions, whilst others have unique molecular component contributions from both ion species. A further breakdown of the PAC classes by ion species, and in terms of numbers of molecular components and class signal intensity contributions, can be found in Fig. S2, supplementary information. Examples of peaks in the 45 cm sample (+) APPI mass spectrum are provided in Fig. 3, which shows four condensed aromatic assignments at lower mass defect (between $m/z$ 432.05 and 432.20), and three example uncondensed molecular assignments at $m/z > 432.20$. Corresponding expansions from the 17.5 cm and 2.5 cm mass spectra are also provided to demonstrate how PAC signal contributions diminish up the sediment core (Fig. 3).

Except for the chlorine-containing classes, Fig. 2 shows that more unique molecular PAC components were detected at the 45 cm depth than for the rest of the core, closely followed by the 35 cm depth, which relate to the 1950s and 1960s, respectively. It is worth noting that the signal intensity contributions from the PAHs (HC) were nearly two fold greater at the 45 cm depth than the 35 cm depth (Fig. S2, supplementary information), which indicates a higher relative abundance of PAHs associated with the 1950s. Domestic coal consumption was widespread in London in the 1950s, and coal-fired power generation occurred within London's urban reaches [3,4]. Although the Great Smog of 1952 provided the impetus for the 1956 Clean Air Act, focusing on coal use and the reduction of 'black smoke' [2], the situation did not improve rapidly enough to avoid another smog event in 1962, resulting in c.750 deaths [1]. Vane et al. suggested that the peak 16 USEPA PAH concentrations in the Chiswick cores likely relate to this period of elevated coal consumption [4], and the same explanation could therefore account for the PAC components observed via (+)APPI-FTICR MS.

The numbers of molecular components for the PAH and NSO-PAC species decreased up the core from the 45 cm depth, with a slight deviation at the 12.5 cm depth for PAHs and $S_1$-PACs (Fig. 2). This

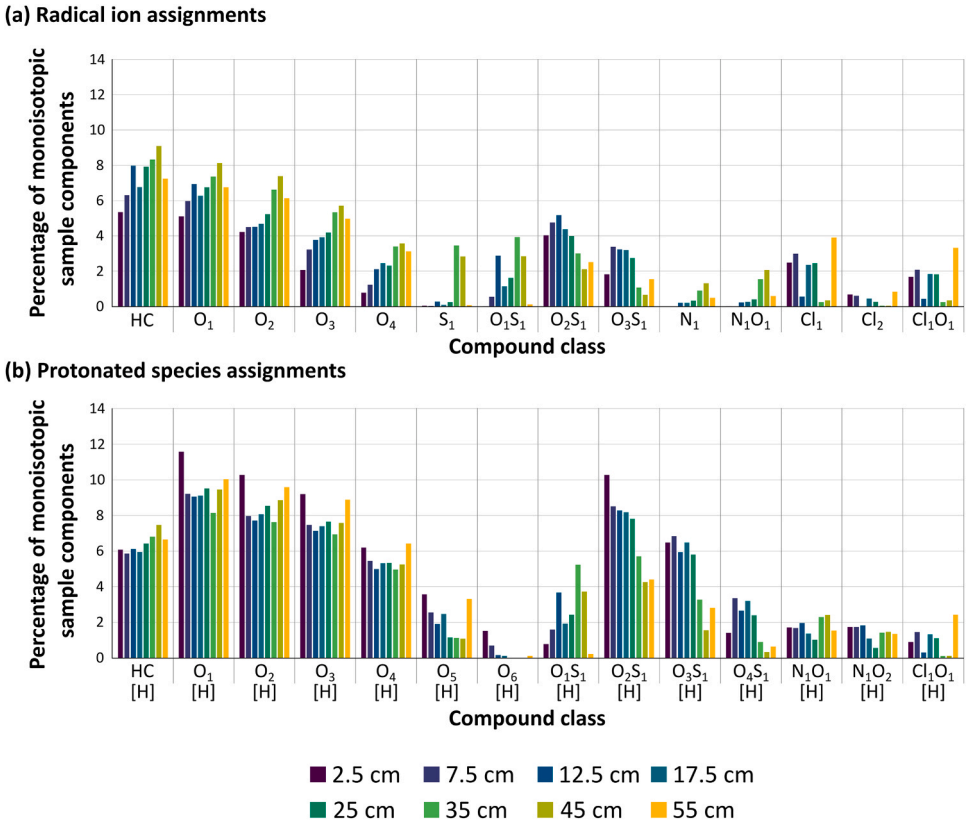


**Fig. 1.** (+)APPI-FTICR MS class distribution for all sediment sample depths (2.5 – 55 cm), separated into the radical ion assignments (a), and protonated species assignments (b).

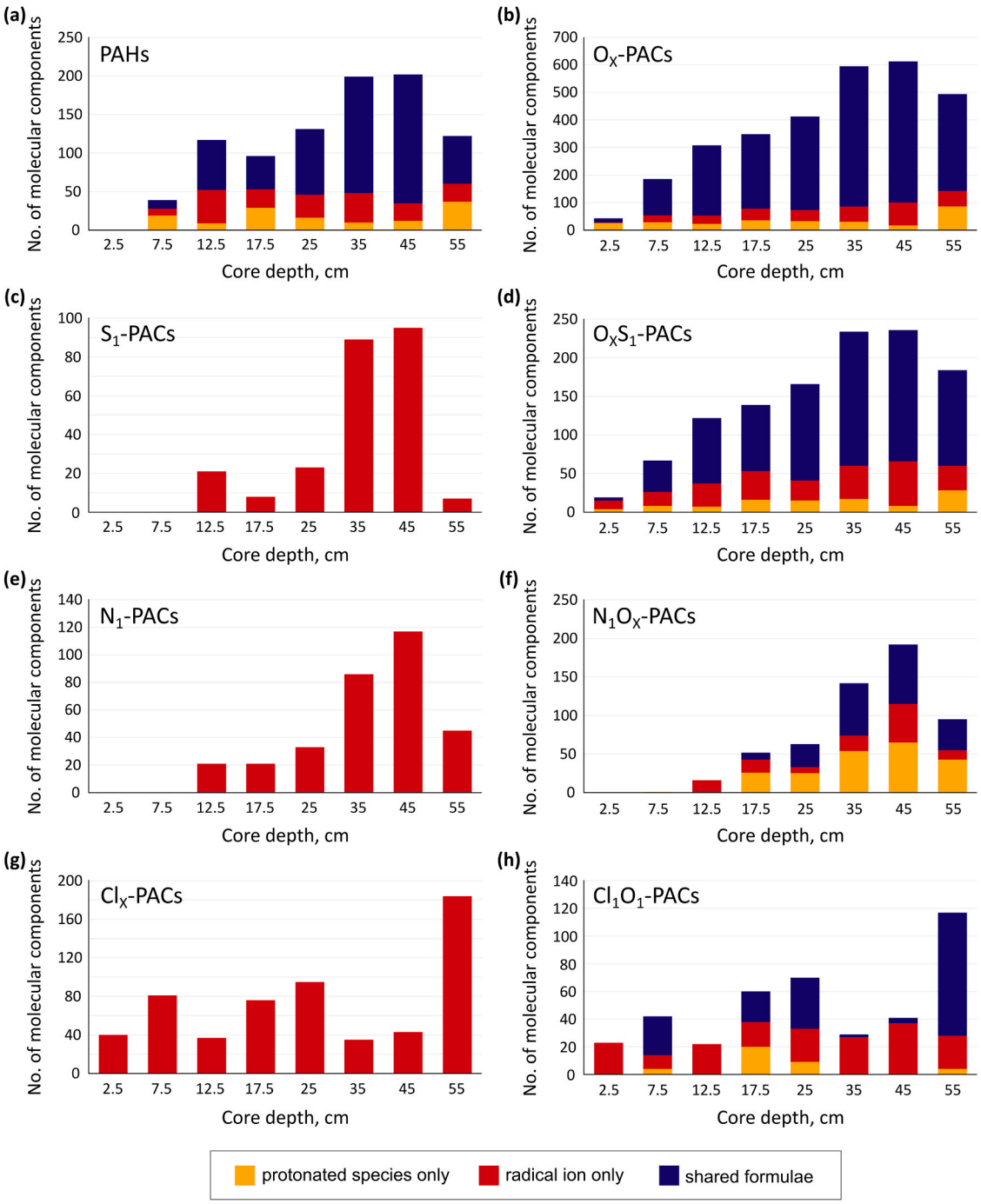


**Fig. 2.** Numbers of unique PAC molecular formulae (AI ≥ 0.67) by class / grouped classes in the (+)APPI data, showing contributions from the two ion species detected: (a) HC and HC[H], (b) $O_1$–$O_4$ and $O_1$[H]–$O_5$[H], (c) $S_1$, (d) $O_1S_1$–$O_3S_1$ and $O_1S_1$[H]–$O_4S_1$[H], (e) $N_1$, (f) $N_1O_1$ and $N_1O_1$[H]–$N_1O_2$[H], (g) $Cl_1$–$Cl_2$, and (h) $Cl_1O_1$ and $Cl_1O_1$[H]. N.B. the y-axes have inconsistent scales for trend clarity.

deviation might relate to a noted rise in emissions from motor vehicles beginning around 1985 [2]. Fig. 4 further presents the total numbers of PACs (AI ≥ 0.67) detected via (+)APPI for each depth, in terms of unique molecular components by analyte compound class, with a maximum of 1538 for the 45 cm depth, or the 1950s. The overall PAC profile trends are broadly consistent with and complement the USEPA 16 PAH quantifications performed by Vane et al. on the same sediment core (Fig. 4) [4]. The decline in PAC components up the core likely relates to the closure of many urban power stations in the 30 years following the Great Smog [3], and the transition away from coal as a domestic fuel, perhaps in combination with other legislative and environmental management-related factors [4]. Coal consumption data for the UK, covering the period relevant to this study, is also shown in Fig. 4, to highlight the proposed connection between the peak in coal consumption during this time and the maximum number of PAC components detected.

The leading hypothesis of a coal related explanation for the sediment core PACs must be accompanied by acknowledgment of other possible source contributions. These include emissions from oil-fuelled power stations (which replaced coal) and other industrial facilities [71,72]. As alluded to, traffic is also a likely factor, especially considering that Chiswick Ait is located close to the Hogarth Roundabout (on the busy A4

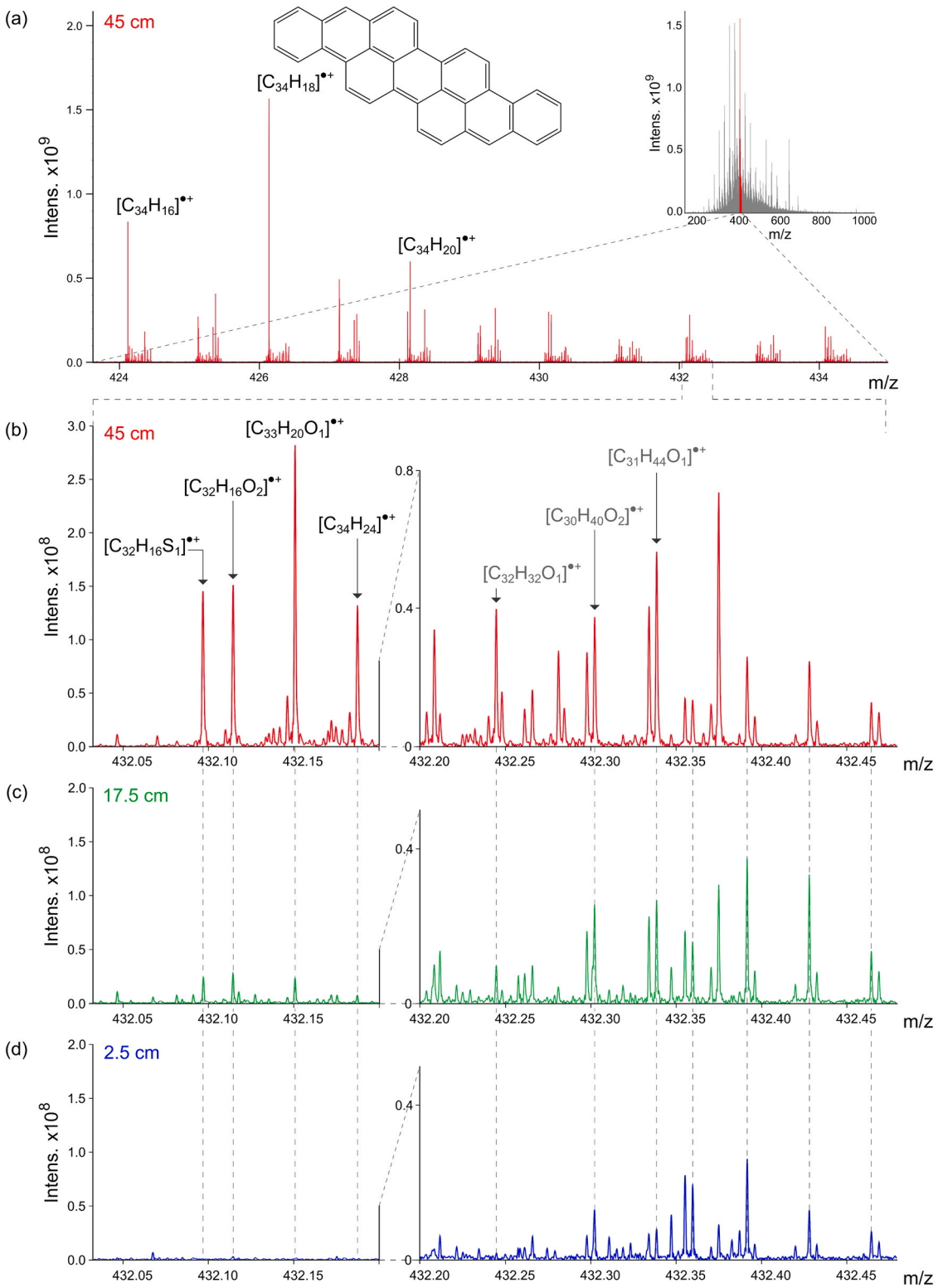


**Fig. 3.** (a) overview of the 45 cm sample (+)APPI-FTICR mass spectrum, with a 10 Da expansion, and a possible structure for the $[C_{34}H_{18}]^{\bullet+}$ ion provided. (b) 0.5 Da expansion of the 45 cm sample spectrum, with four example condensed aromatic ion formulae (annotated), between *m/z* 432.05 and 432.20. Corresponding expansions from the 17.5 cm and 2.5 cm sample mass spectra are provided in (c) and (d), respectively.

road), with tyre wear, asphalt wear, and exhaust particulates representing possible PAC sources [73]. Furthermore, Chiswick Ait is situated near to the outfall from Mogden Sewage treatment works (1939-present day) [7], which may have represented a variable source of PACs from urban runoff or stormwater over the decades.

### 3.3. *DBE versus carbon number plots and PAC structural insights*

Plots of DBE versus carbon number for the (+)APPI HC and $O_1$ radical classes (generally associated with the most PAC components) are provided in Fig. 5, for each sample depth. Each data point represents an

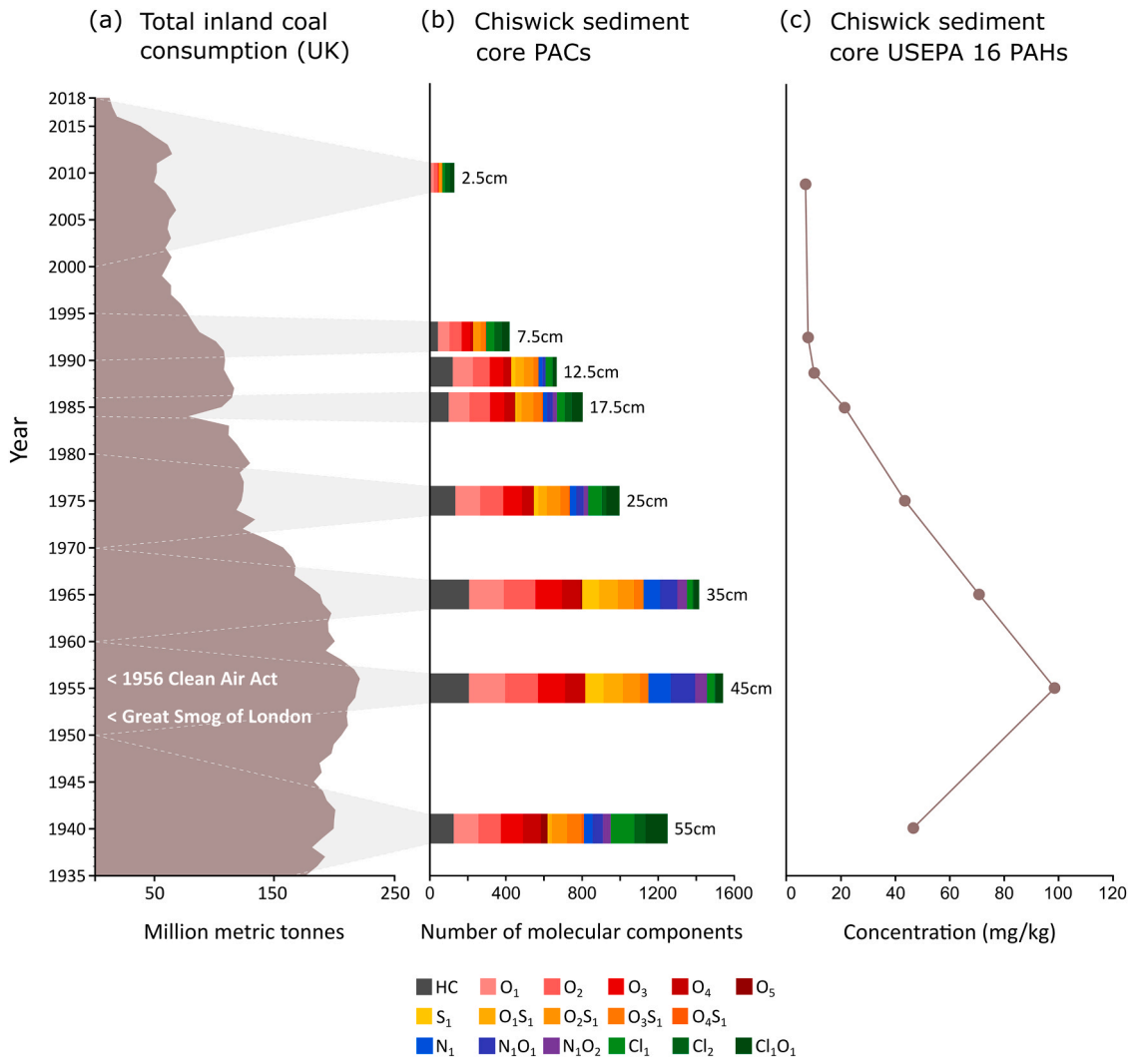


**Fig. 4.** (a) UK coal consumption data [70]. (b) Total PAC molecular components (AI $\geq$ 0.67, monoisotopic) via (+)APPI-FTICR MS, with colours indicating analyte compound classes. (c) Sum USEPA 16 PAH concentrations as determined by Vane et al. [4].

assigned molecular composition, and hence these plots are a means of visualising all mass spectral peaks assigned to a compound class. Most of the molecular formulae distributions in Fig. 5 could be considered bimodal, with an oval distribution below DBE c.15 – 20, with a carbon number range of c.20 – 60, and a more linear, angled distribution sloping up to higher DBE. These linear, angled distributions reflect high molecular condensation, as reported in other FT mass spectrometry pollution-related investigations [44,52–56]. The condensed molecular distributions are a distinctive feature for the 12.5 to 55 cm sample depths, broadly increasing in length and intensity down to the 45 cm depth, before diminishing slightly at the bottom (Fig. 5). The DBE versus carbon number plots for the (+)APPI HC[H] and $O_1$[H] classes (protonated) showed similar condensed molecular distributions to those in the radical classes (Fig. 5), although the data points were typically less intense and distributions were slightly less extensive (examples have been incorporated into Fig. S3, supplementary information). Further examples of similar core profile trends in condensed molecular distributions are presented in DBE versus carbon number plots for the (+)APPI $O_2$ – $O_4$ classes in the supplementary information (Fig. S4).

Connecting the outermost datapoints in the angled, linear distributions yields straight lines which indicate the maximum DBE per carbon number boundary. The theoretical maximum slope of this line for fossil hydrocarbons is the 'planar limit', where DBE equals 90% carbon number (i.e., a gradient of 0.9) [74–76]. Gradients of 0.75 are indicative of cata-condensation; molecular series growth via the linear addition of fused benzene rings, resulting in carbon atoms being shared between no more than two rings [44,76]. Planar limit gradients tending to 1 correspond to peri-condensation, where molecular series growth occurs via non-linear benzene ring addition, allowing for carbon atoms to be shared between three or more rings [44,76]. Herein, best fit lines were constructed for the high molecular condensation distributions in the DBE versus carbon number plots (guided by the more intense data points, as per other work [44]). The gradients were determined to be greater than 0.73 for the relevant (+)APPI compound classes at each sample depth, for both ion types (see Table S3, supplementary information). Furthermore the slopes for many of the classes in the Chiswick core sediment samples were at or above 0.80 (with none greater than 0.86), which is indicative of cata-condensation with contributions from peri-condensed PACs, as has been similarly observed in APPI-FTICR MS data for PACs in atmospheric particulate matter [54]. These gradients may also be consistent with coal asphaltenes, which have been indicated as more enriched in cata-condensed over peri-condensed structures [77].

In the DBE versus carbon number plot for the HC class at a depth of 45 cm, the most intense data points in the condensed molecular distribution occur at carbon number 32 and DBE 25, and carbon number 34 and DBE 26, which likely represents unalkylated PAH compounds with 9 – 10 fused benzene rings. The compounds towards the top-end of the

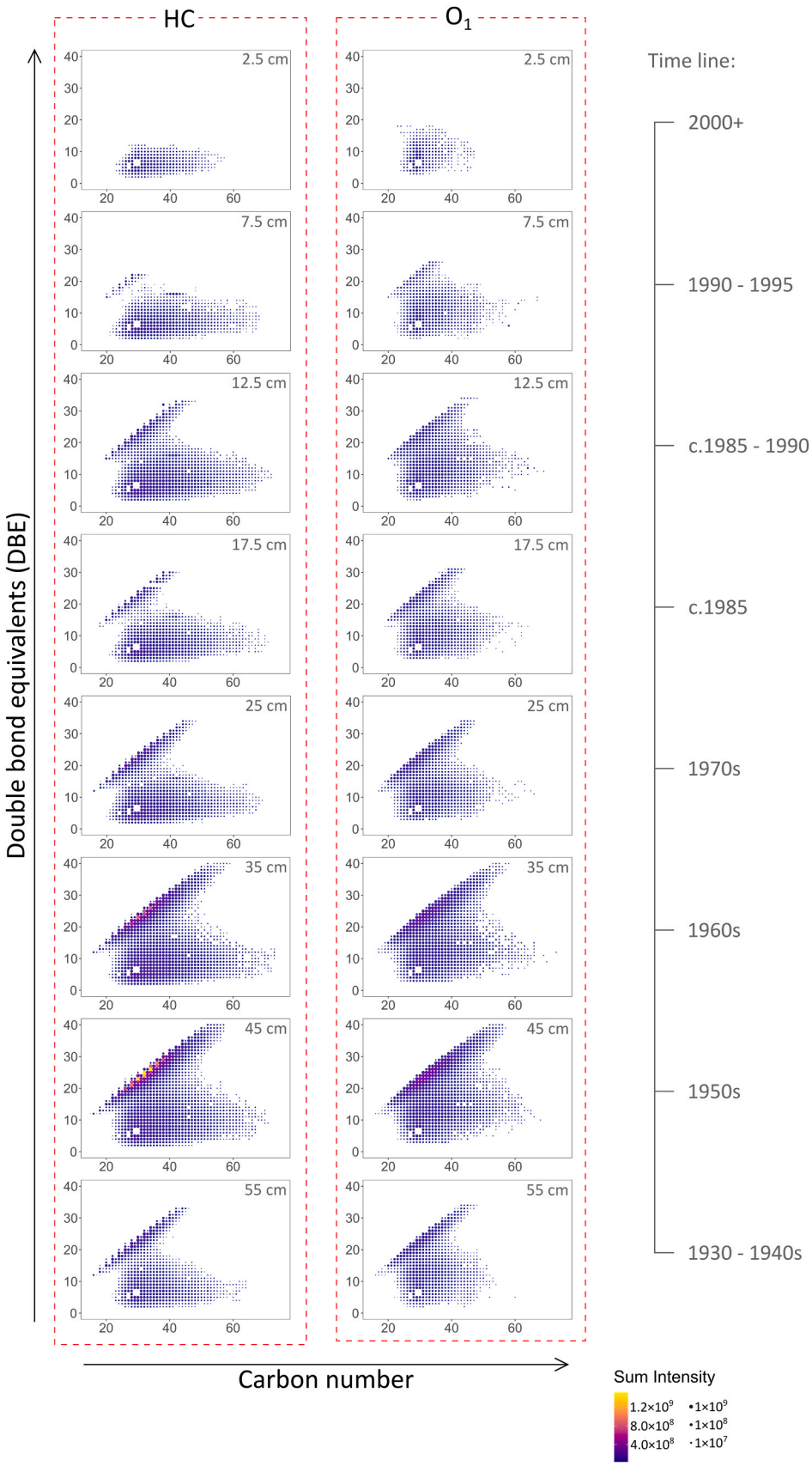


**Fig. 5.** DBE versus carbon number plots for the HC and $O_1$ (radical) ion classes for each sediment core depth, (+)APPI-FTICR MS analysis. Chronology determined by Vane et al. [7].

distribution (e.g., carbon number 52 and DBE 40) are interpreted as PAHs with 15 or more fused benzene rings. Recent observations by Ruiz-Morales indicate that PAH moieties with 8–9 fused aromatic rings are most abundant in soot asphaltene distributions, whereas peak abundance is centred on 7–8 fused aromatic rings for coal asphaltenes and 6–7 fused aromatic rings for petroleum asphaltenes [38]. This suggests that the most abundant contributions to the Chiswick Ait PAH distribution at the 45 cm depth could be more consistent with a soot origin.

Fig. 6 illustrates how the linear, angled distributions in the DBE versus carbon number plots for example (+)APPI radical ion classes relate to condensed and uncondensed aromatic compounds, as calculated via AI. Hence Fig. 6 highlights the PAC distributions in relation to the other compositions in the classes shown, and in some cases the PAC distributions represent the whole class (e.g., $Cl_1$ in Fig. 6), or were separate from the rest of the class data (e.g., $S_1$ in Fig. 6). This could be indicative of a different origin for these condensed aromatic compounds.

The DBE versus carbon number plots contain further information indicative of the origin of the assigned PACs. The length of homologous series (horizontal rows) is representative of the degree of side-chain alkylation occurring [78], and generally it is understood that PACs from petrogenic sources feature greater alkylation than those from pyrogenic sources [12,23]. This was demonstrated using FTICR MS by Rüger et al., who detected a shift in alkylation level to lower carbon number in combustion aerosol compounds compared to parent diesel fuel compounds [78]. Investigating the PAHs associated with soot particles generated in a fuel-rich ethylene flame, using matrix-assisted laser desorption/ionization FTICR MS, Zhang et al. showed a PAH distribution with short homologous series, of no more than four data points per DBE (c.14 – 50) [79]. This indicates limited alkyl side-chain growth for these combustion-source PAHs [79]. Analysing ambient aerosol fractions from Beijing, Jiang et al. detected PAH distributions with narrow homologous series of 5–6 carbon numbers via (+)APPI-FTICR MS, inferring a likely coal-combustion origin [52]. Jiang et al. also reported very similar distributions for related $O_1$, $O_2$, $N_1$ and $S_1$ classes [52]. Regarding the complex PAC mixtures observed in contaminated industrial soil, Luo and Schrader inferred side-chains of 0–10 carbon atoms to be short, and indicative of pyrogenic origin, rather than biogenic or petrogenic [44].

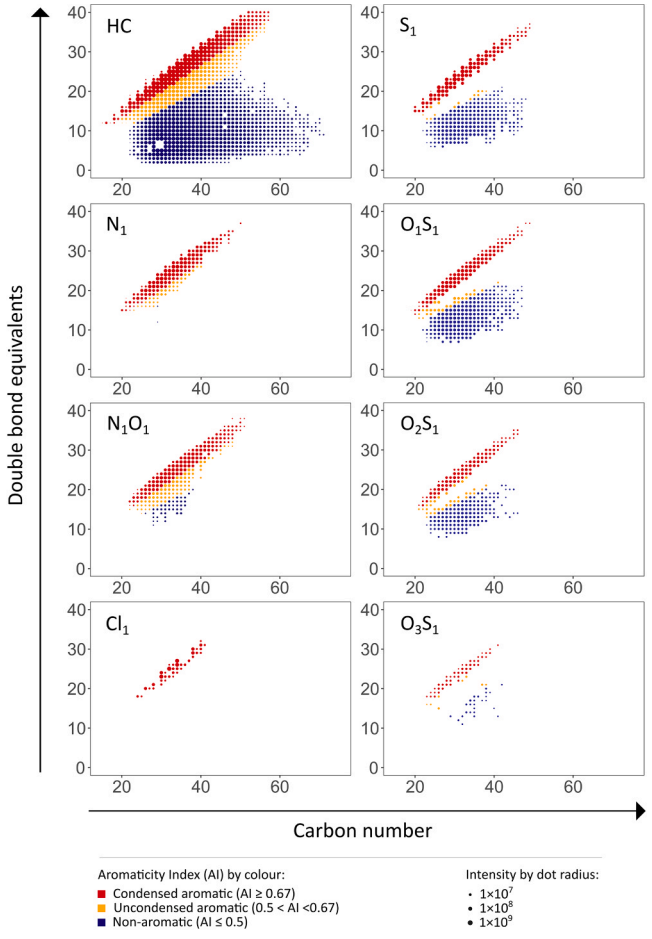


**Fig. 6.** DBE versus carbon number plots for selected (+)APPI radical ion compound classes HC, $N_1$, $N_1O_1$, $Cl_1$, $S_1$, $O_1S_1$, $O_2S_1$ and $O_3S_1$, for the 45 cm sample depth. Datapoints are coloured to reflect AI values.

Fig. 6 hence provides possible evidence for a combustion source origin for the Chiswick Ait PACs at the 45 cm depth, given that most of the PAC-related homologous series are relatively short. In particular, the $Cl_1$ class only has 1–5 datapoints per DBE, and the $S_1$ and $O_xS_1$ classes generally have just 2–5 datapoints in their condensed aromatic distributions – all suggesting very limited PAC alkylation. The $N_1$ class features slightly longer homologous series, with upwards of 9–10 datapoints per row, whereas the $N_1O_1$ class has longer homologous series still, below DBE of c.25. From the $N_1O_1$ class, it can be seen how a homologous series can transition from condensed aromatic species through to non-aromatics (Fig. 6). More extensive examples of longer homologous series stemming from the PAC distribution can be seen in the HC data in Fig. 6, which suggests that this class is not pyrogenic in origin. A few short PAC homologous series do occur in the HC class data for some of the other core depths, but this is limited to higher DBE only (Fig. 5). The $O_X$ classes similarly have mostly longer homologous series, covering broad carbon number ranges (Fig. 5 and Fig. S4, supplementary information).

Although the PAC homologous series in the HC and $O_X$ classes are longer than the other heteroatom classes shown in Fig. 6., the data points are typically intense at or close to the start (left hand side) of homologous series and diminish with increasing alkylation. This intensity trend conveys that more abundant contributions had lower degrees of alkylation, which could be evidence of pyrogenic origin [12,23] or possibly reflect greater contributions of pyrogenic origin PACs co-occurring with compounds from another source.

As aforementioned, some PACs may be regarded as asphaltenes. Recent (+)APPI-FTICR MS work by Niles et al. demonstrates how different asphaltene fraction species from a standard coal can have variable homologous series lengths, with the selected solvent for extraction exerting influence [77]. Hence, the above observations on the potential pyrogenic origin for the Chiswick Ait condensed aromatic compositions should be taken as indicative.

### 3.4. PAHs

The majority of PAHs occurring in urban soils and sediments are expected to be petrogenic or pyrogenic in origin [11,23]. The greatest numbers of PAH molecular components detected in the Chiswick Ait sediments via (+)APPI-FTICR MS was 202 for the 45 cm depth and 199 for the 35 cm depth, coinciding with the 1950s and 1960s, a time where coal dependence caused soot-related smog events [80]. Alongside domestic coal sources, there were multiple former energy installations within a 5 km radius of Chiswick Ait, including the Barnes, Hammersmith, Wandsworth, Fulham and Lombard Road coal-fired power stations, and Brentford gas works [81]. It is therefore likely that coal use is mostly responsible for the PAHs observed for the 45 cm and 35 cm depths. Spatio-temporal variations in combustion temperature, coal rank [82], and industrial capacity could have impacted the complexity of the environmental PAH signatures which, coupled with the influence of the tide on sediment and pollutant distribution, presents interpretive challenges. However, beyond the 1960s, the decline in complex PAH molecular components up the Chiswick core seems broadly reflective of the diminishing coal consumption data for the UK (Fig. 4), if indeed this can be taken to be representative of the Chiswick area. Coal use in

London likely dropped off more sharply than the national trend, as coal power generation remained important in rural locations, but PAH emissions would have continued from other sources, including vehicular emissions.

Soot particles were an important component of London smogs [80], and their close association with PAHs is revealed in considering the pyrolysis of coal in fuel-rich conditions [83–85]. Primary coal pyrolysis generates gases, char and tar, the latter of which contains organic compounds including PAHs, which are either cracked into radicals before polymerising, or are otherwise directly involved in polymerization reactions [85–87]. In particular, fossil fuel pyrolysis produces acetylene which forms and grows smaller PAHs, via various proposed mechanisms [84]. The growth of PAHs leads to irregular graphene layers which cluster, forming soot particles [88]. Other PAHs in the gaseous phase at high temperatures may condense upon cooling onto soot particles [83], if not released directly. It follows that the emission of soot particles and PAHs is linked, and that soot particles are a means for the transport and deposition of PAHs in the environment [83,88]. As aforementioned, the intensity maximum in the 45 cm depth PAH class distribution of condensed aromatics may be indicative of soot asphaltenes [38].

In addition to PAH contamination from incomplete combustion and airborne settlement, the transport and storage of coal and coal combustion residues is presumed to have also contributed towards the complex PAC signature in the Chiswick sediments [89–92]. Many of the aforementioned industrial facilities were located close to the River Thames, and processes such as wind-entrainment and urban run-off present possible direct contaminant delivery mechanisms.

Like PAHs, the heteroatom-containing PACs and/or asphaltenes in coal may have also been involved in soot-forming processes. Kurian et al. observed that the pyrolysis of oil sands asphaltenes formed soot via a mechanism similar to coal pyrolysis [87]. However, coal asphaltenes have not been studied extensively [93], and information concerning soot formation from asphaltenes in general is scarce [87]. As postulated for the PAHs, coal PACs and/or asphaltenes may have also contributed to the complex PAC distributions detected in the Thames sediments more directly, e.g., via wind-blown raw coal dust.

### 3.5. Oxygen-containing PACs (O-PACs)

O-PACs are defined here as compounds with fused aromatic rings and one or more oxygen atoms, meeting the condition AI $\geq$ 0.67. Complex mixtures of such species have recently been reported in aerosol particulate matter from urban and suburban environments [52,53].

O-PACs are thought to form both directly via incomplete fuel combustion, and through secondary reactions in the atmosphere, between PAHs and hydroxyl radicals or ozone molecules [88,94,95]. Oxygen is the most abundant heteroatom in coals [85,96], and O-PACs in coal occur as furans [97] or with ketone, alcohol, or quinone functionalities [52]. Investigating the PACs released on burning low-grade coal (lignite) via fluidised bed combustion, Stefanova et al. detected O-PACs with mono-ketone functionality, anthraquinones, phenols, and furans [98]. Wang et al. also demonstrated that mono-ketones and anthraquinones were emitted when burning coal in domestic stoves [99]. Although these targeted studies are informative, they unlikely represent the full range of structural possibilities for complex mixtures of O-PACs.

Collectively, the O-PAC group represented the largest number of PAC molecular components observed for each Chiswick sediment core depth via (+)APPI (Fig. 2 and Fig. 4). Aromatic alcohols, aldehydes, ketones, esters and oxygen-heterocycles are compounds established to be accessible via (+)APPI, and thus could all be present in the O-PAC classes [100–102]. The sample depths associated with most PAH molecular components also had the greatest numbers of O-PACs (Fig. 2 and Fig. 4). The angled, condensed distributions in the (+)APPI HC class DBE versus carbon number plots are very similar to the corresponding $O_1$ class condensed distributions at each depth, in terms of the DBE and carbon number ranges, and regions of greatest intensity (Fig. 5). The same can be said for the (+)APPI HC[H] and $O_1$[H] classes (as per the example in Fig. S3, supplementary information), thus, the $O_1$-PACs could represent oxidized PAHs, perhaps through in-flame processes or secondary environmental oxidation. A potential oxidation relationship between HC and $O_1$ class PACs was also noted by Jiang et al. [52] and by Xu et al. [54] in their APPI-FTICR MS aerosol particulate matter studies. It follows that the more highly oxygenated Chiswick sediment O-PAC classes could reflect further oxidation of $O_1$-PACs.

O-PACs were further detected through (-)nESI analysis (see supplementary information) of the Chiswick sediments. Via (-)nESI, PACs with one oxygen atom, presumably representing phenolic functionality, provided a minor contribution to the 35 cm and 45 cm depths only (Fig. S5, supplementary information). PACs with two to four oxygen atoms were more significant species (Fig. S5, supplementary information), likely reflecting PACs with multiple alcohol groups, carboxylic acid functionality, or hydroxyfurans [103]. The lower numbers of O-PAC molecular components detected via (-)nESI compared with (+)APPI – 127 versus 612 (AI $\geq$ 0.67) for the 45 cm depth, respectively – suggests that polar, acidic O-PACs are less abundant species in the Chiswick sediments. However, this could simply reflect increased mobility of polar compounds in the riverine environment. Only 38 of the (-)nESI O-PAC molecular formulae were not detected via (+)APPI, however, the 89 molecular formulae commonly detected by both ionization approaches may differ structurally.

### 3.6. Sulfur-containing PACs (S/SO-PACs)

S-PACs are defined here as compounds with fused aromatic rings and a sulfur atom, meeting the condition AI $\geq$ 0.67, and SO-PACs are similar sulfur-containing species which also include one or more oxygen atoms. Polycyclic thiophenes are important S-PAC representatives in fuels such as coal and crude oil (with some dependence on maturity) [96,103], and hence they act as marker compounds in environmental studies, for instance; benzothiophenes and dibenzothiophenes are associated with diesel combustion [69] and petroleum-related contamination [104]. Stefanova et al. demonstrated the emission of S-heterocyclic PAC structures, including dibenzothiophenes and benzonaphthothiophenes, via lignite combustion [98]. Complex distributions of S-PACs have also been reported in ambient aerosol samples of urban origin [52], and sulfur-containing compositions with DBEs up to c.60 have been observed in contaminated industrial soil [44].

The S-PACs in the Chiswick sediment core, only detected as radical ions, occur in notably higher numbers of molecular components in the 45 and 35 cm depths (Fig. 2), with 95 and 89 PACs, respectively, relating to the 1950s and 1960s, when coal combustion had a strong impact on the environment. The S-PAC signal contributions were approximately two times greater in the 45 cm sample than the 35 cm sample, which is indicative of greater relative abundance associated with the 1950s, as was also observed for the PAHs (Fig. S2, supplementary information). London soot particles from 1955 were revealed to contain significant amounts of sulfur via electron microscopy analyses by Whittaker et al., which was attributed to sulfur-rich coal combustion [80]. The S-PAC class in the Chiswick sediments, interpreted here as S-heterocycles, can be taken with Whittaker et al.'s insights [80] to be consistent with the entwined genesis of PACs and soot particles, and their co-emission.

A close similarity exists between the $S_1$ and $S_1O_1$ class DBE versus carbon number distributions, as per the example for the 45 cm depth (Fig. 6), and a general core trend correlation was evident between S-PACs and $S_1O_1$-PAC numbers, indicating that the latter could represent oxidation of the former. The core trends for $S_1O_2$-PACs and $S_1O_3$-PACs were different, showing a gradual increase in components with core depth, and a closer relation to the PAH core profile. The $S_1O_4$-PAC class was minor, with no more than 14 molecular components at any depth. Whilst the $S_1O_2$-, $S_1O_3$- and $S_1O_4$-PACs potentially represent further oxidation of S-heterocyclic PACs, for instance, in the atmosphere, they

may have also been produced from PAHs or O-PACs in the environment. Recently, the formation of organic sulfur compounds was demonstrated following the irradiation of an aqueous solution of simple PAHs with simulated sunlight in the presence of sulfur dioxide (and dimethylsulfoxide) [105]. This represents the environmental scenario of organic sulfur formation at the surface of water bodies, where PAHs can become enriched and react with $SO_2$ released from fossil fuel combustion [105]. Although the study only modelled three parent PAHs, a complex range of possible reactions was unveiled. In particular, Jiang et al. suggested that the direct addition of sulfur dioxide to carbon-carbon double bonds is valid for PAHs in this scenario [105].

The S- and SO-PACs detected in the Chiswick core sediments also show a similar speciation to the sulfur-containing asphaltene compounds recently determined for Illinois Coal No. 6 extracts, via (+)APPI-FTICR MS [77]. Niles et al. reported condensed molecular distributions for $S_1$ and $S_1O_1$-$S_1O_3$ classes, with variations by solvent fractions [77]. It is not possible to infer whether such asphaltene species are contributing to the Chiswick sediments, offering an additional or alternative explanation to secondary reactions between combustion products and atmospheric gases. If the S- and SO-PACs in the Chiswick sediments include coal asphaltene compounds, then this could also be explained by direct contamination of the river Thames by coal dust and/or coal tar. The degree to which coal asphaltenes classes are modified during pyrolysis has not been investigated, to the authors' knowledge.

### 3.7. Nitrogen-containing PACs (N/NO-PACs)

The N-PACs described here feature a nitrogen atom and fused aromatic rings, with AI $\geq$ 0.67, and NO-PACs are similar nitrogen-containing compounds but also with one or more oxygen atoms included. The occurrence of N-PACs and NO-PACs in the environment has been linked to fossil fuel industrial operations and consumption [43,106,107]. The N-PAC heterocycles associated with coal include pyrrolic and pyridinic compounds [97], and in coal tar specifically, the predominant N-PACs are thought to include pyridines and quinolines (basic species), and carbazoles and indoles (neutral species) [103]. Investigating domestic coal combustion, Wang et al. demonstrated the emission of nitro-PACs, which are PAHs with the addition of one or more nitro groups [99]. Nitro-PACs have seen some focus in environmental studies [108] (and references therein), as exemplar compounds possess increased toxicity over parent PAHs [24,107,108]. In addition to the combustion of carbonaceous materials, nitro-PACs can be created in the atmosphere, following reactions between PAHs and OH radicals, nitrogen oxides and ozone [107]. Complex mixtures of N- and/or NO-PACs, extending beyond the nitro subclass, have been reported in FTICR MS aerosol particulate matter research [52–54,56].

The N-PACs in the Chiswick sediment core, only detected as radical ions, show a depth profile similar to the S-PACs: no N-PAC components occurred in the uppermost depths, and notably higher numbers of components were detected in the 45 and 35 cm depths (117 PACs and 86 PACs, respectively, Fig. 2), or the 1950s and 1960s, when coal combustion was elevated (Fig. 4). The N-PAC signal contributions were also approximately two times greater in the 45 cm sample than the 35 cm sample, which indicates greater abundance for the 1950s, as was observed for the S-PACs and PAHs (Fig. S2, supplementary information). The N-PACs are interpreted as likely N-heterocycles, with pyrrole or pyridine moieties fused to benzene rings.

The close appearance between the $N_1$ and $N_1O_1$ class DBE versus carbon number distributions, as per the example for the 45 cm depth (Fig. 6), suggests that the latter class could largely represent oxidation of the former class. This is supported by a general correlation between the N-PACs and $N_1O_1$-PAC molecular component number profiles for the core. The core trends for $N_1O_2$-PACs were similar, but lower numbers of molecular components were represented. It thus seems plausible that the $N_1O_2$-PACs observed via (+)APPI reflect further oxidation of $N_1O_1$-PACs. The $N_1O_2$-PAC class could include nitro-PACs, which have been detected in aerosol particulate matter via (+)APPI previously [56], but these polar species can be water soluble, and hence may not have become sediment-compartmentalised.

NO-PACs were also detected via (-)nESI analysis of the Chiswick sediments (see supplementary information), as species with 1–5 oxygen atoms (Fig. S6, supplementary information). These NO-PACs were mostly associated with the 35 cm and 45 cm depths, but were also observed in the 17.5 cm, 25 cm and 55 cm depths to varying, but overall lesser, degrees. Pyrrole-based structures could ionize via the loss of a proton, and indeed have been inferred in other negative-mode ESI studies of complex organic mixtures [103]. However, if the oxygen atoms are accounted for by OH groups, then this could also explain detection via (-)nESI, and broadens the presence of nitrogen to include possible pyridine moieties. The numbers of NO-PAC molecular components detected via (-)nESI was 143 for the 45 cm sample, which is less that the 192 NO-PACs plus 117 N-PACs observed at this depth via (+)APPI. However, 100 of the NO-PACs detected by (-)nESI were unique molecular formulae, not detected by (+)APPI.

The N- and NO-PACs detected in the Chiswick core sediments further demonstrate similar speciation to asphaltene compounds determined for Illinois Coal No. 6 extracts, where Niles et al. showed condensed molecular distributions for $N_1$ and $N_1O_1$-$N_1O_4$ classes [77]. Asphaltenes from coal and tar thus represent another possible interpretation for the N- and NO-PACs observed in the Chiswick core. Is not possible to suggest whether such compounds could be delivered to the river via the combustion product–airborne settlement route, or whether more direct contamination by coal dust, tar or other residues is a more realistic pathway.

### 3.8. Chlorine-containing PACs (Cl/ClO-PACs)

Cl-PACs are defined here as possessing fused aromatic rings and one to two chlorine atoms, with the AI $\geq$ 0.67 criterion, and ClO-PACs are similar compounds but with only one chlorine and one oxygen atom. The occurrence of chlorine-containing PACs in environmental matrices was realised in the 1980s [109], however, they are still regarded as a new, emerging class of contaminant [110,111]. Cl-PACs have been ascribed to coal combustion, industrial processes, waste incineration, and vehicular emissions [110,112,113]. Coals contain variable quantities of chlorine in different modes [114], which is released during pyrolysis as HCl and, potentially, as chlorinated hydrocarbons [114,115]. Coal ash may also be enriched in chlorine relative to the parent fuel [114]. Cl-PACs are suggested to form from PAHs exposed to HCl in furnaces [111], photochemical reactions with Cl radicals in the atmosphere [111], or aqueous reactions with $Cl_2$ or $ClO_2$ disinfectants [116]. In broad terms, and based on a few low molecular weight class representatives, the occurrence of chlorinated PACs in surface sediments is thought to rise with increasing degree of urbanisation [117].

The presence of chlorine-containing PACs was confirmed for the Chiswick sediment samples via inspection of the distinctive fine isotope patterns they produced in the mass spectra (an example is provided in Fig. S7, supplementary information), and these could be observed due to the ultrahigh-resolving power capabilities of the FTICR mass analyser. The possibility of the detected Cl- and ClO-PAC ions arising due to analyte-solvent (i.e., dichloromethane) interactions was considered, however, this was thought unlikely because the chlorine-containing PAC core profile trends did not reflect the PAH or O-PAC trends (Fig. 2.). Instead, the greatest numbers of molecular Cl- and ClO-PAC components were detected in the 55 cm sample, which features around 40% fewer PAH components than the 45 cm and 35 cm samples (Fig. 2). The numbers of Cl- and ClO-PACs in the 45 cm and 35 cm samples were also substantially fewer than at four other depths (Fig. 2). Various studies have identified correlations between concentrations of targeted chlorinated PACs and their parent PAHs in environmental matrices [110,118], with interpretation of common source. Others, however, have determined no such correlation, indicating that chlorinated PACs and PAHs

originate from different activities [110,117]. The results for the Chiswick sediment core, introducing a more complex mixture perspective, suggest no clear correlation for this study environment.

It is challenging to explain the stronger contributions from chlorinated PACs at some Chiswick sediment depths than at others. There may have been local industrial activities or waste disposal occurrences over the decades that account for these compositions. The incident of a large industrial fire at a plastics plant in Hamilton, Ontario, U.S. in 1997 presents an interesting case of a single release event of chlorinated (and brominated) PACs [119]. Fernando et al. used FTICR MS to detect 150 halogenated PAC molecular formulae in soil samples recovered from the Hamilton site [119]. As discussed, Chiswick Ait is in close proximity to the outfall from the Mogden Sewage treatment works [7], and there is evidence for moderate contributions of treated sewage in the sediments [4]. The use of chlorine as a disinfectant during sewage processing could have potentially generated chlorinated PACs [120]. Indeed, Wang et al. reported the prevalence of Cl-PAHs (low molecular weight) in sewage treatment plant effluent from a facility in Pingdingshan, Henan Province, China [121]. It is therefore possible that sewage treatment activities account for some of the chlorinated PAC contributions in the Chiswick Ait sediments.

The risks to the environment and health presented by Cl-PACs has attracted growing interest [122], with investigations into smaller, exemplar compounds of the class revealing demonstrable carcinogenic and mutagenic properties [111]. Recently Li et al. further provided direct evidence for Cl-PAH immunotoxicity, based on two low molecular weight class representatives [123]. Although not thoroughly assessed and understood, the toxicity associated with chlorinated PACs could be similar to polychlorinated dibenzo-p-dioxins and dibenzofurans [112, 122,124].

It is important to highlight that the chlorinated PAC ions detected for the Chiswick Ait sediments correspond to compositions with around 4–14 fused aromatic rings, and to the authors' knowledge no specific information is available regarding the genesis, environmental fate, or toxicity of the medium to larger molecular weight species within the detected range.

## 4. Conclusions

Organic extracts from a Chiswick Ait sediment core from the River Thames, London, covering a time period from the 1930s to 2018, were analysed using an untargeted broadband (+)APPI-FTICR mass spectrometry approach, with additional insights on highly polar compositions gathered via (-)nESI-FTICR MS. Using complex mixture analysis techniques, involving DBE versus carbon number plots and aromaticity index calculations, it was possible to gain molecular compositional insights corresponding to PACs in the sediments, and show the variations in PAC distributions as a function of sediment core depth. The greatest number of unique PAC molecular formulae detected was for the 45 cm depth, which corresponds to the 1950s. This included 1406 PACs (of which 202 were PAHs) only detected via (+)APPI, 138 PACs only detected via (-)nESI, and an additional 132 PACs detected by both ionization methods. The condensed aromatic compositions included those with oxygen, sulfur, nitrogen and chlorine heteroatoms. Given London's coal dependence during the 1950s, these complex PAC mixtures are largely attributed to the products of incomplete coal combustion and direct coal material contamination scenarios. Specific features in the data are indicative of pyrogenic contributions, and a possible soot association. The compound classes observed are also relatable to those reported for aerosol particulate matter and coal asphaltenes in the literature.

The PAC contributions to the sediments as assessed by FTICR MS likely included contributions from other sources, such as vehicle emissions. However, the numbers of PAC molecular components were shown to decline up the sediment core overall, which likely reflects the transition towards cleaner fuels and de-industrialisation efforts in London since the 1960s. This decline is related to the concentrations of USEPA 16 PAHs determined for the same sediment core in an earlier study by Vane et al. [4] Thus, we show that the relative contamination view offered by the USEPA 16 PAH concentrations is indicative of the relative extent of PAC distributions unveiled by FTICR MS.

## Environmental implication

This work concerns polycyclic aromatic compounds (PACs), a contaminant class with exemplar carcinogens and endocrine disruptors. PACs are a concern as they are persistent, and growing evidence shows that they can occur as complex mixtures in the environment. Untargeted ultrahigh-resolution mass spectrometry herein has unveiled complex mixtures of PACs in sediments from the River Thames, London, with temporal variance reflecting historic coal consumption. The numbers of PACs extend far beyond the lists of target compounds that many environmental investigations focus on. The PAC compositional space detected has been speciated across multiple heteroatom classes, providing insights to guide future targeted work.

## CRediT authorship contribution statement

**Mark P Barrow:** Writing – review & editing, Supervision, Resources, Methodology, Funding acquisition, Conceptualization. **Hugh Jones:** Writing – review & editing. **Christopher Vane:** Writing – review & editing, Supervision, Resources, Methodology, Funding acquisition, Conceptualization. **Benedict Gannon:** Writing – review & editing, Visualization, Software. **Diana Catalina Palacio Lozano:** Writing – review & editing. **Rory Downham:** Writing – review & editing, Writing – original draft, Visualization, Methodology, Investigation, Formal analysis, Data curation, Conceptualization.

## Declaration of Competing Interest

The authors declare the following financial interests/personal relationships which may be considered as potential competing interests: Rory Downham reports financial support was provided by Natural Environment Research Council. Benedict Gannon reports financial support was provided by Natural Environment Research Council. Hugh Jones reports financial support was provided by Engineering and Physical Sciences Research Council. Diana Catalina Palacio Lozano reports financial support was provided by Leverhulme Trust. Christopher Vane reports financial support was provided by British Geological Survey. Mark Barrow reports financial support was provided by Warwick Innovations (University of Warwick). Mark Barrow reports software was provided by Sierra Analytics, Inc.

## Data availability

Data will be made available on request.

## Acknowledgements

The authors thank the Natural Environment Research Council (NERC) for PhD studentships funded via the Central England NERC Training Alliance (CENTA) (grant numbers NE/L002493/1 and NE/S007350/1), and the Engineering and Physical Sciences Research Council (EPSRC) for a PhD studentship through the EPSRC Centre for Doctoral Training in Molecular Analytical Science (grant number EP/L015307/1). The Leverhulme Trust is thanked for providing an Early Career Fellowship (ECF-2020–393), and Warwick Innovations is thanked for funding in the development of KairosMS. This project was also funded in part by the British Geological Survey, Organic Geochemistry Facility, NE4699S and BUFI, S436. C. H. Vane publishes with permission of the Director of the British Geological Survey. The authors further thank David Stranz (Sierra Analytics) for collaborative

developments and access to Composer software.

## Appendix A. Supporting information

Supplementary data associated with this article can be found in the online version at doi:10.1016/j.jhazmat.2024.134605.

## References


[1] Met Office, ⟨https://www.metoffice.gov.uk/weather/learn-about/weather/case-studies/great-smog⟩, (accessed June 2022).
[2] Longhurst, J.W.S., Barnes, J.H., Chatterton, T.J., Hayes, E.T., Williams, W.B., 2016. Progress with air quality management in the 60 years since the UK Clean Air Act, 1956. Lessons, failures, challenges and opportunities. Int J Sustain Dev Plan 11, 461–499.
[3] Fowler, D., Brimblecombe, P., Burrows, J., Heal, M., Grennfelt, P., Stevenson, D., et al., 2020. A chronology of global air quality. Philos Trans R Soc, A 378, 20190314.
[4] Vane, C.H., Kim, A.W., Lopes dos Santos, R.A., Moss-Hayes, V., 2022. Contrasting sewage, emerging and persistent organic pollutants in sediment cores from the river thames estuary, London, England, UK. Mar Pollut Bull 175, 113340.
[5] Bai, X., McPhearson, T., Cleugh, H., Nagendra, H., Tong, X., Zhu, T., et al., 2017. Linking urbanization and the environment: conceptual and empirical advances. Annu Rev Environ Resour 42, 215–240.
[6] Taylor, K., Owens, P., 2009. Sediments in urban river basins: a review of sediment-contaminant dynamics in an environmental system conditioned by human activities. J Soils Sediment 9, 281–303.
[7] Vane, C.H., Turner, G.H., Chenery, S.R., Richardson, M., Cave, M.C., Terrington, R., et al., 2020. Trends in Heavy Metals, Polychlorinated Biphenyls and Toxicity from Sediment Cores of the Inner River Thames Estuary, London, UK. Environ Sci: Process Impacts 22, 364–380.
[8] Bertrand, O., Mondamert, L., Grosbois, C., Dhivert, E., Bourrain, X., Labanowski, J., et al., 2015. Storage and Source of Polycyclic Aromatic Hydrocarbons in Sediments Downstream of a Major Coal District in France. Environ Pollut 207, 329–340.
[9] Park, J.-H., Penning, T.M., 2008. In: Stradler, R.H., Lineback, D.R. (Eds.), Polyaromatic Hydrocarbons, in *Process-Induced Food Toxicants: Occurrence, Formation, Mitigation, and Health Risks*, 1st edn.,. John Wiley & Sons Ltd, New Jersey, pp. 243–282. ch. 2h.
[10] Poster, D., Schantz, M., Sander, L., Wise, S., 2006. Analysis of Polycyclic Aromatic Hydrocarbons (PAHs) in Environmental Samples: a critical review of gas chromatographic (GC) Methods. Anal Bioanal Chem 386, 859–881.
[11] Srogi, K., 2007. Monitoring of environmental exposure to polycyclic aromatic hydrocarbons: a review. Environ Chem Lett 5, 169–195.
[12] Andersson, J., Achten, C., 2015. Time to Say Goodbye to the 16 EPA PAHs? Toward an Up-to-Date Use of PACs for Environmental Purposes. Polycycl Aromat Compd 35, 330–354.
[13] Keith, L., 2015. The Source of US EPA's Sixteen PAH Priority Pollutants. Polycyclic Aromat Compd 35, 147–160.
[14] Patel, A., Shaikh, S., Jain, K., Desai, C., Madamwar, D., 2020. Polycyclic aromatic hydrocarbons: sources, toxicity, and remediation approaches. Front Microbiol 11, 562813.
[15] Parker, D., Zhang, F., Kim, Y., Kaiser, R., Landera, A., Kislov, V., et al., 2012. Low temperature formation of naphthalene and its role in the Synthesis of PAHs (Polycyclic Aromatic Hydrocarbons) in the interstellar medium. Proc Natl Acad Sci USA 109, 53–58.
[16] Du, J., Jing, C., 2018. Anthropogenic PAHs in lake sediments: a literature review (2002-2018). Environ Sci: Process Impacts 20, 1649–1666.
[17] Mojiri, A., Zhou, J., Ohashi, A., Ozaki, N., Kindaichi, T., 2019. Comprehensive review of polycyclic aromatic hydrocarbons in water sources, their effects and treatments. Sci Total Environ 696, 133971.
[18] Sander, L.C., Schantz, M.M., Wise, S.A., 2017. Environmental Analysis: Persistent Organic Pollutants. In: Fanali, S., Haddad, P.R., Poole, C.F., Riekkola, M.-L. (Eds.), Liquid Chromatography, 2nd edn.,. Elsevier, pp. 401–449. ch. 14.
[19] Honda, M., Suzuki, N., 2020. Toxicities of polycyclic aromatic hydrocarbons for aquatic animals. Int J Environ Res Public Health 17, 1363.
[20] Zhang, Y., Dong, S., Wang, H., Tao, S., Kiyama, R., 2016. Biological Impact of Environmental Polycyclic Aromatic Hydrocarbons (ePAHs) as Endocrine Disruptors. Environ Pollut 213, 809–824.
[21] Das, S., Routh, J., Roychoudhury, A., 2008. Sources and historic changes in polycyclic aromatic hydrocarbon input in a Shallow Lake, Zeekoevlei, South Africa. Org Geochem 39, 1109–1112.
[22] Ravindra, K., Sokhi, R., Van Grieken, R., 2008. Atmospheric Polycyclic Aromatic Hydrocarbons: Source Attribution, Emission Factors and Regulation. Atmos Environ 42, 2895–2921.
[23] Stout, S., Emsbo-Mattingly, S., Douglas, G., Uhler, A., McCarthy, K., 2015. Beyond 16 Priority Pollutant PAHs: a review of PACs used in Environmental Forensic Chemistry. Polycycl Aromat Compd 35, 285–315.
[24] B.-K. Lee, Sources, Distribution and Toxicity of Polyaromatic Hydrocarbons (PAHs) in Particulate Matter, in *Air Pollution*, ed. V. Villanyi, IntechOpen, London, UK, 1st edn, 2010, ch. 5, doi:10.5772/10045.
[25] Han, J., Liang, Y., Zhao, B., Wang, Y., Xing, F., Qin, L., 2019. Polycyclic Aromatic Hydrocarbon (PAHs) Geographical Distribution in China and their Source, Risk Assessment Analysis. Environ Pollut 251, 312–327.
[26] Menichini, E., Bocca, B., 2003. Polycyclic Aromatic Hydrocarbons. In: Trugo, L., Finglas, P.M. (Eds.), Encyclopedia of food sciences and nutrition, 2nd edn.,. Elsevier Science Ltd., pp. 4616–4625
[27] Beriro, D., Cave, M., Kim, A., Craggs, J., Wragg, J., Thomas, R., et al., 2020. Soil-Sebum Partition Coefficients for High Molecular Weight Polycyclic Aromatic Hydrocarbons (HMW-PAH). J Hazard Mater 398, 122633.
[28] Long, A., Lemieux, C., Gagne, R., Lambert, I., White, P., 2017. Genetic toxicity of complex mixtures of polycyclic aromatic hydrocarbons: evaluating dose-additivity in a transgenic mouse model. Environ Sci Technol 51, 8138–8148.
[29] Manzano, C., Hoh, E., Simonich, S., 2013. Quantification of complex polycyclic aromatic hydrocarbon mixtures in standard reference materials using comprehensive two-dimensional gas chromatography with time-of-flight mass spectrometry. J Chromatogr A 1307, 172–179.
[30] Achten, C., Andersson, J., 2015. Overview of Polycyclic Aromatic Compounds (PAC). Polycycl Aromat Compd 35, 177–186.
[31] Hodson, P., Wallace, S., de Solla, S., Head, S., Hepditch, S., Parrott, J., et al., 2020. Polycyclic Aromatic Compounds (PACs) in the Canadian Environment: the challenges of ecological risk assessments. Environ Pollut 266, 115165.
[32] Andersson, J., Hegazi, A., Roberz, B., 2006. Polycyclic aromatic sulfur heterocycles as information carriers in environmental studies. Anal Bioanal Chem 386, 891–905.
[33] Witter, A., Nguyen, M., 2016. Determination of Oxygen, Nitrogen, and Sulfur-Containing Polycyclic Aromatic Hydrocarbons (PAHs) in Urban Stream Sediments. Environ Pollut 209, 186–196.
[34] Han, Y., Wei, C., Huang, R., Bandowe, B., Ho, S., Cao, J., et al., 2016. Reconstruction of atmospheric soot history in inland regions from lake sediments over the past 150 years. Sci Rep 6, 19151.
[35] Shiraiwa, M., Selzle, K., Poschl, U., 2012. Hazardous components and health effects of atmospheric aerosol particles: reactive oxygen species, soot, polycyclic aromatic compounds and allergenic proteins. Free Radic Res 46, 927–939.
[36] Alostad, L., Lozano, D., Gannon, B., Downham, R., Jones, H., Barrow, M., 2022. Investigating the influence of n-Heptane versus n-Nonane upon the Extraction of Asphaltenes. Energy Fuels 36, 8663–8673.
[37] Ruiz-Morales, Y., 2007. Molecular Orbital Calculations and Optical Transitions of PAHs and Asphaltenes. In: Mullins, O.C., Sheu, E.Y., Hammami, A., Marshall, A.G. (Eds.), in *Asphaltenes, Heavy Oils, and Petroleomics*, 1st edn.,. Springer, New York, pp. 95–137. ch. 4.
[38] Ruiz-Morales, Y., 2022. Application of the Y-Rule and Theoretical Study to Understand the Topological and Electronic Structures of Polycyclic Aromatic Hydrocarbons from Atomic Force Microscopy Images of Soot, Coal Asphaltenes, and Petroleum Asphaltenes. Energy Fuels 36, 8725–8748.
[39] Schuler, B., Meyer, G., Pena, D., Mullins, O., Gross, L., 2015. Unraveling the molecular structures of asphaltenes by atomic force microscopy. J Am Chem Soc 137, 9870–9876.
[40] Hall, R., Wolfe, B., Wiklund, J., Edwards, T., Farwell, A., Dixon, D., 2012. Has alberta oil sands development altered delivery of polycyclic aromatic compounds to the peace-athabasca delta? PLoS One 7, e46089.
[41] Han, Y., Wei, C., Bandowe, B., Wilcke, W., Cao, J., Xu, B., et al., 2015. Elemental Carbon and Polycyclic Aromatic Compounds in a 150-Year Sediment Core from Lake Qinghai, Tibetan Plateau, China: influence of Regional and Local Sources and Transport Pathways. Environ Sci Technol 49, 4176–4183.
[42] Han, Y., Bandowe, B., Schneider, T., Pongpiachan, S., Ho, S., Wei, C., et al., 2021. A 150-Year Record of Black Carbon (Soot and Char) and Polycyclic Aromatic Compounds Deposition in Lake Phayao, North Thailand. Environ Pollut 269, 116148.
[43] Chibwe, L., Roberts, S., Shang, D., Yang, F., Manzano, C., Wang, X., et al., 2020. A one-century sedimentary record of N- and S-Polycyclic Aromatic Compounds in the Athabasca Oil Sands Region in Canada. Chemosphere 260, 127641.
[44] Luo, R., Schrader, W., 2021. Getting a Better Overview of a Highly PAH Contaminated Soil: a non-targeted approach assessing the real environmental contamination. J Hazard Mater 418, 126352.
[45] Smith, D., Podgorski, D., Rodgers, R., Blakney, G., Hendrickson, C., 2018. 21 Tesla FT-ICR Mass Spectrometer for Ultrahigh-Resolution Analysis of Complex Organic Mixtures. Anal Chem 90, 2041–2047.
[46] Lozano, D., Gavard, R., Arenas-Diaz, J., Thomas, M., Stranz, D., Mejia-Ospino, E., et al., 2019. Pushing the analytical limits: new insights into complex mixtures using mass spectra segments of constant ultrahigh resolving power. Chem Sci 10, 6966–6978.
[47] Kim, S., Rodgers, R., Marshall, A., 2006. Truly "Exact" Mass: elemental composition can be determined uniquely from molecular mass measurement at ~0.1 mDa Accuracy for Molecules up to ~500 Da. Int J Mass Spectrom 251, 260–265.
[48] Palacio Lozano, D., Thomas, M.J., Jones, H.E., Barrow, M.P., 2020. Petroleomics: tools, challenges, and developments. Annu Rev Anal Chem 13, 405–430.
[49] Marshall, A., Rodgers, R., 2008. Petroleomics: Chemistry of the Underworld. Proc Natl Acad Sci USA 105, 18090–18095.
[50] McLafferty, F.W., Turecek, F., 1993. Elemental Composition. In: McLafferty, F.W., Turecek, F. (Eds.), in *Interpretation of Mass Spectra*, 4th edn.,. University Science Books, Mill Valley, pp. 19–34. ch. 2.
[51] Lin, P., Fleming, L., Nizkorodov, S., Laskin, J., Laskin, A., 2018. Comprehensive molecular characterization of atmospheric brown carbon by high resolution mass spectrometry with electrospray and atmospheric pressure photoionization. Anal Chem 90, 12493–12502.

[52] Jiang, B., Liang, Y., Xu, C., Zhang, J., Hu, M., Shi, Q., 2014. Polycyclic Aromatic Hydrocarbons (PAHs) in Ambient Aerosols from Beijing: Characterization of Low Volatile PAHs by Positive-Ion Atmospheric Pressure Photoionization (APPI) Coupled with Fourier Transform Ion Cyclotron Resonance. Environ Sci Technol 48, 4716–4723.
[53] Choi, J., Ryu, J., Jeon, S., Seo, J., Yang, Y., Pack, S., et al., 2017. In-Depth Compositional Analysis of Water-Soluble and -Insoluble Organic Substances in Fine (PM2.5) Airborne Particles Using Ultra-High Resolution 15T FT-ICR MS and GCx GC-TOFMS. Environ Pollut 225, 329–337.
[54] Xu, C., Gao, L., Zheng, M., Qiao, L., Wang, K., Huang, D., et al., 2021. Nontarget screening of polycyclic aromatic compounds in atmospheric particulate matter using ultrahigh resolution mass spectrometry and comprehensive two-dimensional gas chromatography. Environ Sci Technol 55, 109–119.
[55] Kim, D., Kim, S., Yim, U., Ha, S., An, J., Loh, A., et al., 2022. Determination of anthropogenic organics in dichlomethane extracts of aerosol particulate matter collected from four different locations in China and Republic of Korea by GC-MS and FTICR-MS. Sci Total Environ 805, 150230.
[56] Kuang, B., Yeung, H., Lee, C., Griffith, S., Yu, J., 2018. Aromatic Formulas in Ambient PM2.5 Samples from Hong Kong Determined Using FT-ICR Ultrahigh-Resolution Mass Spectrometry. Anal Bioanal Chem 410, 6289–6304.
[57] Marshall, A., Hendrickson, C., 2008. High-resolution mass spectrometers. Annu Rev Anal Chem 1, 579–599.
[58] Gavard, R., Jones, H., Lozano, D., Thomas, M., Rossell, D., Spencer, S., et al., 2020. KairosMS: a new solution for the processing of hyphenated ultrahigh resolution mass spectrometry data. Anal Chem 92, 3775–3786.
[59] Jones, H., Lozano, D., Huener, C., Thomas, M., Aaserud, D., DeMuth, J., et al., 2021. Influence of biodiesel on base oil oxidation as measured by FTICR Mass Spectrometry. Energy Fuels 35, 11896–11908.
[60] Lozano, D., Jones, H., Gavard, R., Thomas, M., Ramirez, C., Wootton, C., et al., 2022. Revealing the Reactivity of Individual Chemical Entities in Complex Mixtures: the Chemistry Behind Bio-Oil Upgrading. Anal Chem 94, 7536–7544.
[61] Koch, B.P., Dittmar, T., 2006. From Mass to Structure: an aromaticity index for high-resolution mass data of natural organic matter. Rapid Commun Mass Spectrom 20, 926–932.
[62] Koch, B., Dittmar, T., 2016. From Mass to Structure: an aromaticity index for high-resolution mass data of natural organic matter (Vol 20, pg 926, 2006). Rapid Commun Mass Spectrom 30, 250-250.
[63] Wang, X., Wang, J., Zhang, Y., Shi, Q., Zhang, H., Zhang, Y., et al., 2016. Characterization of Unknown Iodinated Disinfection Byproducts During Chlorination/Chloramination Using Ultrahigh Resolution Mass Spectrometry. Sci Total Environ 554, 83–88.
[64] Schneider, E., Giocastro, B., Ruger, C., Adam, T., Zimmermann, R., 2022. Detection of polycyclic aromatic hydrocarbons in high organic carbon ultrafine particle extracts by electrospray ionization ultrahigh-resolution mass spectrometry. J Am Soc Mass Spectrom 33, 2019–2023.
[65] Melendez-Perez, J., Martinez-Mejia, M., Eberlin, M., 2016. A reformulated aromaticity index equation under consideration for non-aromatic and non-condensed aromatic cyclic carbonyl compounds. Org Geochem 95, 29–33.
[66] Purcell, J., Hendrickson, C., Rodgers, R., Marshall, A., 2006. Atmospheric pressure photoionization fourier transform ion cyclotron resonance mass spectrometry for complex mixture analysis. Anal Chem 78, 5906–5912.
[67] Thomas, M., Chan, H., Lozano, D., Barrow, M., 2022. Solvent and flow rate effects on the observed compositional profiles and the relative intensities of radical and protonated species in atmospheric pressure photoionization mass spectrometry. Anal Chem 94, 4954–4960.
[68] Thomas, M., Collinge, E., Witt, M., Lozano, D., Vane, C., Moss-Hayes, V., et al., 2019. Petroleomic depth profiling of staten island salt marsh soil: 2 Omega Detection FTICR MS Offers a new solution for the analysis of environmental contaminants. Sci Total Environ 662, 852–862.
[69] Lee, C., Brimblecombe, P., 2016. Anthropogenic Contributions to Global Carbonyl Sulfide, Carbon Disulfide and Organosulfides Fluxes. Earth-Sci Rev 160, 1–18.
[70] Department for Energy Security and Net Zero and Department for Business, ⟨https://www.gov.uk/government/statistical-data-sets/historical-coal-data-coal-production-availability-and-consumption⟩ (accessed June 2023).
[71] Vane, C.H., Kim, A.W., Beriro, D., Cave, M.R., Lowe, S.R., Lopes dos Santos, R.A., et al., 2021. Persistent Organic Pollutants in Urban Soils of Central London, England, UK: Measurement and Spatial Modelling of Black Carbon (BC), Petroleum Hydrocarbons (TPH), Polycyclic Aromatic Hydrocarbons (PAH) and Polychlorinated Biphenyls (PCB). Adv Environ Eng Res 2. https://doi.org/10.21926/aeer.2102011.
[72] Melsted, O., Pallua, I., 2018. The historical transition from coal to hydrocarbons: previous explanations and the need for an integrative perspective. Can J Hist-Ann Can D Hist 53, 395–422.
[73] Grung, M., Lindman, S., Kringstad, A., Girardin, V., Meland, S., 2022. Alkylated polycyclic aromatic compounds in road runoff are an environmental risk and should be included in future investigations. Environ Toxicol Chem 41, 1838–1850.
[74] Purcell, J., Merdrignac, I., Rodgers, R., Marshall, A., Gauthier, T., Guibard, I., 2010. Stepwise structural characterization of asphaltenes during deep hydroconversion processes determined by atmospheric pressure photoionization (APPI) fourier transform ion cyclotron resonance (FT-ICR) mass spectrometry. Energy Fuels 24, 2257–2265.
[75] Hsu, C., Lobodin, V., Rodgers, R., McKenna, A., Marshall, A., 2011. Compositional boundaries for fossil hydrocarbons. Energy Fuels 25, 2174–2178.
[76] Cho, Y., Kim, Y., Kim, S., 2011. Planar limit-assisted structural interpretation of saturates/aromatics/resins/asphaltenes fractionated crude oil compounds observed by fourier transform ion cyclotron resonance mass spectrometry. Anal Chem 83, 6068–6073.
[77] Niles, S., Chacon-patino, M., Smith, D., Rodgers, R., Marshall, A., 2020. Comprehensive compositional and structural comparison of coal and petroleum asphaltenes based on extrography fractionation coupled with fourier transform ion cyclotron resonance MS and MS/MS Analysis. Energy Fuels 34, 1492–1505.
[78] Rüger, C.P., Sklorz, M., Schwemer, T., Zimmermann, R., 2015. Characterisation of ship diesel primary particulate matter at the molecular level by means of ultra-high-resolution mass spectrometry coupled to laser desorption ionisation-comparison of feed fuel, filter extracts and direct particle measurements. Anal Bioanal Chem 407, 5923–5937.
[79] Zhang, W., Shao, C., Sarathy, S.M., 2020. Analyzing the solid soot particulates formed in a fuel-rich flame by solvent-free matrix-assisted laser desorption/ionization fourier transform ion cyclotron resonance mass spectrometry. Rapid Commun Mass Spectrom 34, e8596.
[80] Whittaker, A., BeruBe, K., Jones, T., Maynard, R., Richards, R., 2004. Killer Smog of London, 50 Years On: particle properties and oxidative capacity. Sci Total Environ 334, 435–445.
[81] Industry on the River Thames, Books LLC, Memphis, USA, 2010.
[82] Gao, M., Wang, Y., Dong, J., Li, F., Xie, K., 2016. Release behavior and formation mechanism of polycyclic aromatic hydrocarbons during coal pyrolysis. Chemosphere 158, 1–8.
[83] Wornat, M., Ledesma, E., Sandrowitz, A., Roth, M., Dawsey, S., Qiao, Y., et al., 2001. Polycyclic aromatic hydrocarbons identified in soot extracts from domestic coal burning stoves of Henan Province, China. Environ Sci Technol 35, 1943–1952.
[84] Williams, A., Lea-Langton, A.R., Bartle, K.D., 2021. The Formation of PAH Compounds from the Combustion of Biofuels. In: Gupta, A.K., De, A., Aggarwal, S. K., Kushari, A., Runchal, A.K. (Eds.), in Advances in Energy and Combustion, 1st edn.,. Springer, Singapore, pp. 105–124.
[85] Fletcher, T., Ma, J., Rigby, J., Brown, A., Webb, B., 1997. Soot in coal combustion systems. Prog Energy Combust Sci 23, 283–301.
[86] Liu, G., Niu, Z., Van Niekerk, D., Xue, J., Zheng, L., 2008. Polycyclic Aromatic Hydrocarbons (PAHs) from Coal Combustion: Emissions, Analysis, and Toxicology. In: Whitacre, D.M. (Ed.), Reviews of Environmental Contamination and Toxicology, 1st edn.,, vol. 192. Springer, New York, pp. 1–28.
[87] Kurian, V., Mahapatra, N., Wang, B., Alipour, M., Martens, F., Gupta, R., 2015. Analysis of Soot Formed during the Pyrolysis of Athabasca Oil Sand Asphaltenes. Energy Fuels 29, 6823–6831.
[88] Maranzana, A., Serra, G., Giordana, A., Tonachini, G., Barco, G., Causa, M., 2005. Ozone Interaction with Polycyclic Aromatic Hydrocarbons and Soot in Atmospheric Processes: theoretical density functional study by molecular and periodic methodologies. J Phys Chem A 109, 10929–10939.
[89] Petrovic, M., Fiket, Z., 2022. Environmental damage caused by coal combustion residue disposal: a critical review of risk assessment methodologies. Chemosphere 299, 134410.
[90] Verma, S., Masto, R., Gautam, S., Choudhury, D., Ram, L., Maiti, S., et al., 2015. Investigations on PAHs and Trace Elements in Coal and its Combustion Residues from a Power Plant. Fuel 162, 138–147.
[91] Li, H., Liu, G., Cao, Y., 2014. Content and distribution of trace elements and polycyclic aromatic hydrocarbons in Fly Ash from a Coal-Fired CHP Plant. Aerosol Air Qual Res 14, 1179–1188.
[92] Szatylowicz, E., Walendziuk, W., 2021. Analysis of Polycyclic Aromatic Hydrocarbon Content in Ash from Solid Fuel Combustion in Low-Power Boilers. Energies 14, 6801.
[93] Zhu, Y., Guo, Y., Zhang, X., Tian, F., Luo, C., Du, C., et al., 2022. Exploration of coal tar asphaltene molecules based on high resolution mass spectrometry and advanced extraction separation method. Fuel Process Technol 233, 107309.
[94] Walgraeve, C., Demeestere, K., Dewulf, J., Zimmermann, R., Van Langenhove, H., 2010. Oxygenated polycyclic aromatic hydrocarbons in atmospheric particulate matter: molecular characterization and occurrence. Atmos Environ 44, 1831–1846.
[95] Shen, G., Tao, S., Wang, W., Yang, Y., Ding, J., Xue, M., et al., 2011. Emission of oxygenated polycyclic aromatic hydrocarbons from indoor solid fuel combustion. Environ Sci Technol 45, 3459–3465.
[96] Bartle, K., Hall, S., Holden, K., Mitchell, S., Ross, A., 2009. Analysis of oxygen-containing polycyclic aromatic compounds by gas chromatography with atomic emission detection. Fuel 88, 348–353.
[97] Wang, R., Sun, R., Liu, G., Yousaf, B., Wu, D., Chen, J., et al., 2017. A review of the biogeochemical controls on the occurrence and distribution of polycyclic aromatic compounds (PACs) in coals. Earth-Sci Rev 171, 400–418.
[98] Stefanova, M., Marinov, S., Mastral, A., Callen, M., Garcia, T., 2002. Emission of oxygen, sulphur and nitrogen containing heterocyclic polyaromatic compounds from lignite combustion. Fuel Process Technol 77, 89–94.
[99] Wang, J., Du, W., Chen, Y., Lei, Y., Chen, L., Shen, G., et al., 2022. Nitrated and oxygenated polycyclic aromatic hydrocarbons emissions from solid fuel combustion in rural china: database of 12 real-world scenarios for residential cooking and heating activities. Sci Total Environ 852, 158501.
[100] Kondyli, A., Schrader, W., 2020. Evaluation of the combination of different atmospheric pressure ionization sources for the analysis of extremely complex mixtures. Rapid Commun Mass Spectrom 34, e8676.
[101] Acter, T., Kim, D., Ahmed, A., Jin, J., Yim, U., Shim, W., et al., 2016. Optimization and application of atmospheric pressure chemical and photoionization hydrogen-deuterium exchange mass spectrometry for speciation of oxygen-containing compounds. Anal Bioanal Chem 408, 3281–3293.

[102] Kauppila, T., Kersten, H., Benter, T., 2015. Ionization of EPA Contaminants in Direct and Dopant-Assisted Atmospheric Pressure Photoionization and Atmospheric Pressure Laser Ionization. J Am Soc Mass Spectrom 26, 1036–1045.
[103] Liu, F., Fan, M., Wei, X., Zong, Z., 2017. Application of mass spectrometry in the characterization of chemicals in coal-derived liquids. Spectrom Rev 36, 543–579.
[104] Radovic, J., Xie, W., Silva, R., Oldenburg, T., Larter, S., Zhang, C., 2022. Changes of organic matter composition in surface sediments from the pearl river estuary to the coastal south china sea revealed by rapid molecular screening using FTICR-MS. Org Geochem 173, 104505.
[105] Jiang, H., He, Y., Wang, Y., Li, S., Jiang, B., Carena, L., et al., 2022. Formation of organic sulfur compounds through SO2-Initiated Photochemistry of PAHs and dimethylsulfoxide at the air-water interface. Atmos Chem Phys 22, 4237–4252.
[106] Chibwe, L., Manzano, C., Muir, D., Atkinson, B., Kirk, J., Marvin, C., et al., 2019. Deposition and source identification of nitrogen heterocyclic polycyclic aromatic compounds in snow, sediment, and air samples from the athabasca oil sands region. Environ Sci Technol 53, 2981–2989.
[107] Bandowe, B., Meusel, H., 2017. Nitrated Polycyclic Aromatic Hydrocarbons (Nitro-PAHs) in the Environment - A Review. Sci Total Environ 581, 237–257.
[108] Nowakowski, M., Rykowska, I., Wolski, R., Andrzejewski, P., 2022. Polycyclic Aromatic Hydrocarbons (PAHs) and their Derivatives (O-PAHs, N-PAHs, OH-PAHs): Determination in Suspended Particulate Matter (SPM) - A Review. Environ Process 9. https://doi.org/10.1007/s40710-021-00555-7.
[109] Fu, P., Von Tungeln, L., Chiu, L., Own, Z., 1999. Halogenated-Polycyclic Aromatic Hydrocarbons: a class of genotoxic environmental pollutants. J Environ Sci Health, Part C: Environ Carcinog Ecotoxicol Rev 17, 71–109.
[110] Kamiya, Y., Iijima, A., Ikemori, F., Okuda, T., Ohura, T., 2016. Source apportionment of chlorinated polycyclic aromatic hydrocarbons associated with ambient particles in a Japanese Megacity. Sci Rep 6, 38358.
[111] Vuong, Q., Thang, P., Ohura, T., Choi, S., 2020. Chlorinated and brominated polycyclic aromatic hydrocarbons in ambient air: seasonal variation, profiles, potential sources, and size distribution. Rev Environ Sci Bio/Technol 19, 259–273.
[112] Jin, R., Zheng, M., Lammel, G., Bandowe, B., Liu, G., 2020. Chlorinated and brominated polycyclic aromatic hydrocarbons: sources, formation mechanisms, and occurrence in the environment. Prog Energy Combust Sci 76, 100803.
[113] Eklund, G., Stromberg, B., 1983. Detection of polychlorinated polynuclear aromatics in flue-gases from coal combustion and refuse incinerators. Chemosphere 12, 657–660.
[114] Yudovich, Y., Ketris, M., 2006. Chlorine in coal: a review. Int J Coal Geol 67, 127–144.
[115] Glarborg, P., 2007. Hidden Interactions - Trace Species Governing Combustion and Emissions. Proc Combust Inst 31, 77–98.
[116] Rav-Acha, C., Blits, R., 1985. The different reaction mechanisms by which chlorine and chlorine dioxide react with polycyclic aromatic hydrocarbons (PAH) in Water. Water Res 19, 1273–1281.
[117] Sun, J., Ni, H., Zeng, H., 2011. Occurrence of chlorinated and brominated polycyclic aromatic hydrocarbons in surface sediments in shenzhen, south china and its relationship to urbanization. J Environ Monit 13, 2775–2781.
[118] Horii, Y., Ohura, T., Yamashita, N., Kannan, K., 2009. Chlorinated polycyclic aromatic hydrocarbons in sediments from industrial areas in Japan and the United States. Arch Environ Contam Toxicol 57, 651–660.
[119] Fernando, S., Jobst, K., Taguchi, V., Helm, P., Reiner, E., McCarry, B., 2014. Identification of the Halogenated Compounds Resulting from the 1997 Plastimet Inc. Fire in Hamilton, Ontario, using Comprehensive Two-Dimensional Gas Chromatography and (Ultra)High Resolution Mass Spectrometry. Environ Sci Technol 48, 10656–10663.
[120] Ohura, T., 2007. Environmental behavior, sources, and effects of chlorinated polycyclic aromatic hydrocarbons. Sci World J 7, 372–380.
[121] Wang, X., Kang, H., Wu, J., 2016. Determination of chlorinated polycyclic aromatic hydrocarbons in water by solid-phase extraction coupled with gas chromatography and mass spectrometry. J Sep Sci 39, 1742–1748.
[122] Jin, R., Liu, G., Zheng, M., Fiedler, H., Jiang, X., Yang, L., et al., 2017. Congener-specific determination of ultratrace levels of chlorinated and brominated polycyclic aromatic hydrocarbons in atmosphere and industrial stack gas by isotopic dilution gas chromatography/high resolution mass spectrometry method. J Chromatogr A 1509, 114–122.
[123] Li, X., Ma, M., Zhao, B., Li, N., Fang, L., Wang, D., et al., 2022. Chlorinated polycyclic aromatic hydrocarbons induce immunosuppression in THP-1 macrophages characterized by disrupted amino acid metabolism. Environ Sci Technol 56, 16012–16023.
[124] Ma, J., Chen, Z., Wu, M., Feng, J., Horii, Y., Ohura, T., et al., 2013. Airborne PM2.5/PM10-Associated chlorinated polycyclic aromatic hydrocarbons and their parent compounds in a Suburban Area in Shanghai, China. Environ Sci Technol 47, 7615–7623.